Hindawi
Geofluids
Volume 2022, Article ID 2150607, 22 pages
https://doi.org/10.1155/2022/2150607

Research Article

Extremely High Primary Productivity and Organic Matter Enrichment in Lacustrine Sediments: Late Triassic Chang 7^3 Sub-Member, Western Ordos Basin

Zhiwei Liao, Zigang Wu, Qiang Chen, Yi Zhang, Xiaodong Wang, Yunqian Liu, and Zhijie Xu

State Key Laboratory of Coal Mine Disaster Dynamics and Control, School of Resources and Safety Engineering, Chongqing University, Chongqing 400044, China

Correspondence should be addressed to Qiang Chen; chenqiang2019@cqu.edu.cn

Received 9 August 2022; Revised 23 September 2022; Accepted 28 September 2022; Published 7 October 2022

Academic Editor: Yuxiang Zhang

The 7th member of the Late Triassic Yanchang Formation is the most important Mesozoic source rocks and shale oil reservoir in the Ordos Basin. The hydrocarbon potential and organic matter enrichment mechanism of this organic-rich member are questioned because of the high heterogeneity of continental sediments. In particular, the lack of drilling in the Chang 7^3 sub-member of the western Ordos Basin (central Tianhuan Depression) hinders this understanding and the progress of shale oil exploration in this region. In this study, 87 samples were collected from the well DP1 in the Tianhuan Depression, western Ordos Basin, and analyzed for sedimentology and geochemistry to unravel the paleoenvironment, paleo-productivity, and hydrocarbon potential of the Chang 7^3 sub-member. The results show that the Chang 7^3 shale is characterized by ultra-high organic matter abundance (up to 10.60%), type II kerogen, and good hydrocarbon generation potential. An intermediate chemical weathering intensity suggests that this set of organic-rich shale was deposited in a warm and humid paleoclimate setting. Extreme organic matter enrichment in study area may be attributed to ultra-high productivity (hypereutrophic lake), superimposed terrigenous organic matter input, and transgression, rather than volcanism and anoxic bottom water. This model is different from those of Chang 7^3 interval with higher organic matter content in the central and southern parts of the Ordos Basin. Therefore, this study proposes that the Chang 7^3 shale in the central Tianhuan Depression is not a good target layer for shale oil exploration and that the favorable area may be located in an undisturbed deep lake with higher organic matter abundance (e.g., southwestern Ordos Basin).

1. Introduction

Shale oil is an unconventional oil and gas resource trapped in organic-rich shale rock series, including petroleum resources in shale pores and fractures and the interlayer of carbonate or clastic rocks. Its development can only be realized by using a horizontal well and hydraulic fracturing [1]. Recent shale oil exploration breakthroughs on the Bakken Formation of the Williston Basin, Eagle Ford Formation of South Texas, and Barnett Formation of the Fort Worth Basin in North America have reformed the energy structure of the United States and had a profound impact on the world energy pattern [2–5]. China also pay attention on shale oil and gas resources and made successively discovering in the Permian Lucaogou Formation of the Junggar Basin [6], the Triassic Yanchang Formation in the Ordos Basin [7], the Jurassic Ziliujing Formation in the Sichuan Basin [8], the Cretaceous Qingshankou Formation in the Songliao Basin [9], and the Paleogene Shahejie Formation in the Bohai Bay Basin [10].

The largest shale oilfield in China was discovered in the source rock layer of the Chang 7 member of the Qingcheng area of the Ordos Basin [11]. In a short time period, a million-ton-level shale oil development demonstration base was established, which delivered proven accumulated reserves of 10.52×10^8 t. In 2020, shale oil production in the demonstration area was 93×10^4 t, and the shale oil production in the basin reached 143×10^4 t. Current research showed that the Triassic Yanchang Formation in the Ordos Basin, especially the Chang 7 member, have various favorable geological conditions for large-scale shale oil formation and accumulation, e.g., interbedded of the source rock and reservoir [11]. In addition, the organic-rich shale strata in the Chang 7 member are not only the target layers for shale oil occurrence and exploration but also the material basis for oil and gas generation. As the most important source rock in the Ordos Basin, the dark fine-grained rock of the Chang 7 member has ultra-high organic matter content (up to 30–40%), a large thickness (>80 m), moderate thermal maturity (Ro 0.7–1.1%), a large distribution area ($5 \times 10^4 - 10 \times 10^4$ km^2), and other beneficial characteristics [12], controlling the macroscopic distribution of Mesozoic oil and gas [13]. Previous studies on the Chang 7 member have mainly focused on the paleoclimate [14], redox state [15], paleo-productivity [16], and volcanic eruption events [17] at the time of its deposition. However, lacustrine sediments vary remarkably across basins due to highly heterogeneous sedimentary facies. For reasons such as the distribution of drilling and outcrops in the field, these studies mainly focused on the central and southwestern parts of the basin [18], while the western regions (Tianhuan Depression) of the Chang 7 member, especially the Chang 7^3 sub-member, are less involved [19]. This situation has limited the understanding of the source rock formation characteristics as well as the oil and gas resource potential in these areas. Therefore, it is important to investigate the geological origin of this set of organic-rich rocks to improve future shale oil and gas reserves.

In this study, comprehensive analyses were carried out on the sedimentology, geochemistry, and petroleum geology of the shale cores from the Chang 7^3 sub-member of the Mahuangshan area in the western Ordos Basin to determine the characteristics of source rocks and the mechanism of organic matter enrichment. This study aimed to provide a theoretical foundation for the evaluation of the oil and gas resource potential of the Chang 7^3 sub-member.

2. Geological Background

The Ordos Basin, located in the western North China Block, is a large intra-cratonic basin with an area of approximately 2.5×10^5 km^2. It consists of six first-order tectonic units: the Yishan slope in the center, the Yimeng uplift in the north, the Jinxi flexural-fold belt in the east, the Weibei uplift in the south, the Tianhuan Depression in the west, and the western edge fold-thrust belt uplift in the north ([20]; Figure 1(a)). The tectonic evolution of the Ordos Basin was influenced by the paleo-Asian ocean plate to the north, the Qilian-Qinling trough, and the Helan Aulacogen to the south and southwest [21]. During the Late Triassic era, the Qilian-Qinling tectonic belt experienced rapid uplift caused by the collision of the North and South China blocks [22], resulting in subsidence in the southwest of the basin and the formation of a large depressed lake basin with a wide area. The Late Triassic Yanchang Formation in the Ordos Basin developed an intracontinental fluvial–delta–lacustrine clastic facies, which can be divided into 10 oil-bearing layers in ascending order, corresponding to the process of formation, development, and disappearance of the lake basin (Figure 1(b)). Large-scale lake transgression occurred during the early stages of the Chang 7 period, forming alternating layers of organic-rich black shales and sandstones. The Chang 7 member was principally deposited in a semi-deep–deep lake environment and can be subdivided into three sub-members: Chang 7^3, Chang 7^2, and Chang 7^1, from the bottom to the top. The Chang 7^3 sub-member was deposited in the maximum stage of lake basin evolution, and then the lake basin began to shrink and decrease during the Chang 7^2 period until the center of the lake basin retreated to the Jiyuan, Huachi, and Fuxian areas at the end of the Chang 7^1 interval [23].

The Yanchang Formation in the study area is comparatively well-developed, with a burial depth of 2600–2800 m and a total thickness of approximately 715 m. The exploration well DP1 in this study is located in the western Ordos Basin, in the Ningxia Mahuangshan area, which geologically belongs to the central part of the Tianhuan Depression. The purpose of drilling was to drill through the Chang 7 member and aimed at coring the organic-rich shale of the Chang 7^3 sub-member at a depth from 2743.08 m to 2785.63 m. Previous studies compared [24, 25] the logging in Chang 7^3 with those in Chang 7^2 sub-member and Chang 8 member and characterized Chang 7^3 sub-member by high gamma ray (GR), high acoustic (AC), high induction standard processed resistivity (ILD), and low density (DEN) (Figure 2) [24, 25]. Consequently, this study considers that the cored section is mainly Chang 7^3 sub-member in well DP 1 and 2743.08–2780 m and 2780–2785.63 m are Chang 7^3 sub-member and uppermost Chang 8 member, respectively (Figure 2).

3. Samples and Analytical Methods

87 dark-black organic-rich shale core samples were collected from the Chang 7^3 sub-member ($n = 80$) and Chang 8 member ($n = 7$) of well DP1. These samples were tested for petrologic observations, total organic carbon and sulfur (TOC-TS) content, Rock-Eval pyrolysis, chloroform bitumen "A," vitrinite reflectance (R_o), organic macerals, and major and trace elements. All tests except major and trace elements were carried out at the State Key Laboratory of Oil and Gas Reservoir Geology and Exploitation (Southwest Petroleum University), China. Major and trace elements were analyzed at the Wuhan Sample Solution Analytical Technology Co., Ltd.

The TOC and TS contents were determined using a LECO CS230 carbon-sulfur analyzer, with powdered shale samples passing through a 200-mesh sieve. Before TOC-TS measurement, the sample powder was soaked in diluted 10% hydrochloric acid to dissolve the carbonate minerals, which were subsequently leached with deionized water. The precision of the TOC and TS contents data was better than ±0.02%. The Rock-Eval pyrolysis analysis of the powdered shale samples was carried out using a Rock-Eval 6 analyzer using a temperature-programmed method to

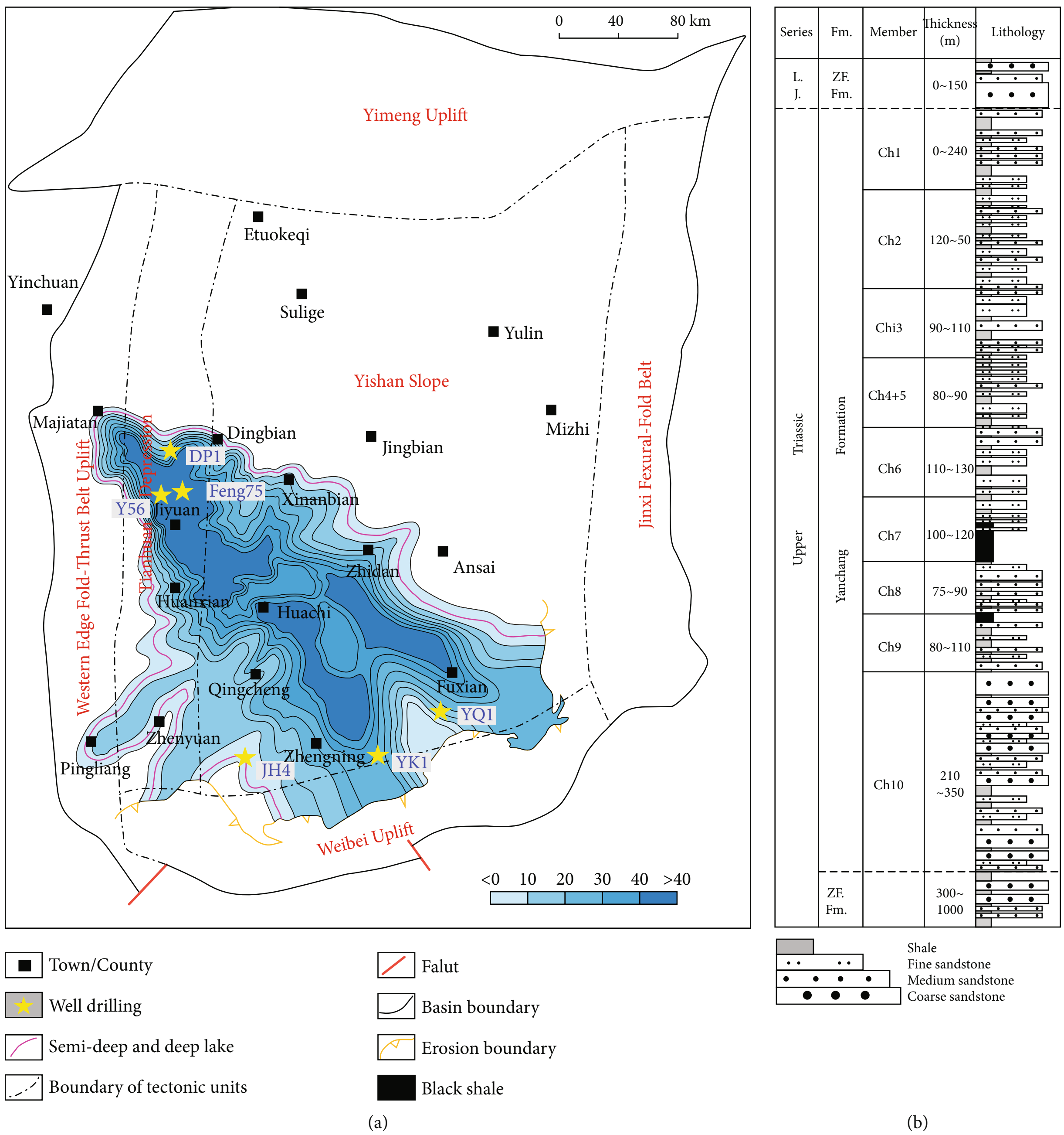

Figure 1: (a) The simplified tectonic map and distribution of Chang 7 members in the Ordos Basin. (b) Stratigraphic column of late Triassic Yanchang Formation in the Ordos Basin. Note that yellow pentagram represents the related drillings in the discussion. This figure is modified from Fu et al. [24].

pyrolyze or thermally evaporate hydrocarbons in the shale at different temperatures. The residual hydrocarbons in the rock were released before the temperature reached 300 °C, and the P_1 peak and the corresponding peak areas (S_1) were measured. The P_2 peak and peak areas (S_2) were measured at temperatures between 300 °C and 500 °C. Usually, S_1 represents the amount of residual hydrocarbons in the samples, and S_2 represents the total amount of hydrocarbons produced from kerogen pyrolysis and extractable heavy components (e.g., gums and asphaltenes).

Chloroform bitumen "A" in shale samples was obtained by extracting soluble organic matter using organic solvents (e.g., chloroform and methanol) and a Soxhlet extractor. The vitrinite reflectance of the shale organic matter was measured using a Leica DM4500P + QDI308 vitrinite reflectance meter. Based on the organic petrology method, the shale samples were ground into a light sheet, and organic macerals were identified using a Leica DM4500P polarizing microscope based on their differences in reflected light characteristics, color, and morphological structure. The whole-rock major and trace element analysis was performed using X-ray fluorescence spectrometry (XRF) and Agilent 7700e quadrupole inductively coupled plasma mass spectrometry (ICP–MS), respectively. Detailed analytical procedures have

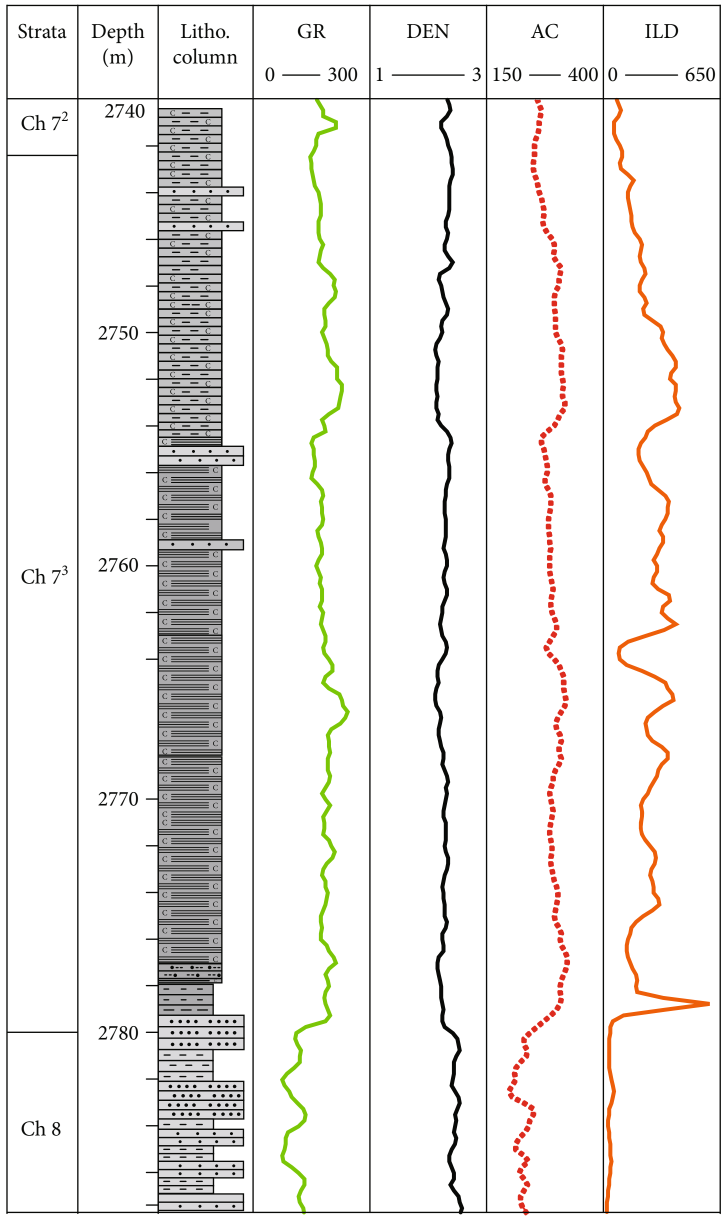

FIGURE 2: Logging profile displaying gamma ray (GR), density (DEN), acoustic (AC), and resistivity (ILD) of Chang 7^3 sub-member from well DP1 in the western Ordos Basin. Note that the logging variations are used for stratigraphic division.

been described by Zhang et al. [26]. Analytical uncertainty was estimated to be less than 10% and 5%, respectively.

4. Results

4.1. Petrological Characteristics. The drilling cores collected in well DP1 were divided into six roundtrips. The 1st to 5th roundtrips (2743.08–2778.06 m) were dominated by gray-black carbonaceous shale (Figure 3(a)) and interbedded with fine sandstone layers of small thickness (Figure 3(c)), and the bedding was well developed. Pyrite nodules (Figure 3(d)) were common, and oil flowers were occasionally observed during core washing. The core fractures were developed with a fluorescence display in the 5th roundtrip. After immersed in water, fish-seed-shaped and needle-shaped air bubbles with diameter of 1–1.5 mm was presented continuously (Figure 3(e)), accounting for approximately 10–20% of the whole section. The 6th roundtrip (2778.18–2785.63 m) was predominantly light gray, medium–fine sandstone in lithology (Figure 3(b)), with low-angle fractures. The yellow crude oil seeped along the natural rock fractures, showing oil traces (Figure 3(f)).

Detailed petrological observations show that the top of the Chang 8 member is composed mainly of medium–fine grained sandstones with a small fraction of dark mudstone (Figure 4(a)). The samples collected in the Chang 7^3 sub-member are fine-grained sedimentary rocks that primarily consist of clay minerals, organic matter, and terrigenous clastic grains such as quartz (Figures 4(b)–4(h)). Fine sandstone is visible in some layers (Figures 3(a) and 3(c)). The

FIGURE 3: Photographs of core from Chang 8 to Chang 7^3 intervals in well DP1. (a) Dark shale interbedded with fine sandstone in the 1^{st} to 5^{th} roundtrips. (b) Gray medium–fine sandstone in the 6^{th} roundtrip. (c) Fine sandstone in the 2^{nd} roundtrip. (d) Pyrite nodules in the 4^{th} roundtrip. (e) Air bubbles occurred in water from the 5^{th} roundtrip. (F) Yellow crude oil seeped in the 6^{th} roundtrip. Note that the yellow arrow in (a) indicates the bottom and top of the drilling core.

upper member of the Chang 7^3 sub-member contains more bio-detritus such as phosphorous biological and spherical fragments (Figures 4(c)–4(e)). In terms of sedimentary structure, most samples show obvious horizontal bedding (e.g., Figures 4(d)–4(f)), while some samples show blocky structures (Figure 4(c)). In the 1^{st} to 5^{th} roundtrips, a large amount of organic matter is distributed in the bedding, and framboidal pyrite particles of less than 7 μm in size were observed under a scanning electron microscope (SEM) (Figure 4(g)). In the 5^{th} roundtrip, tiny cracks (Figure 4(h)) were observed in the shale layer. In conclusion, the lithology of the Chang 7^3 sub-member is mostly gray-black organic-rich shale interbedded with fine sandstone layers, indicating a semi-deep–deep lake environment. This

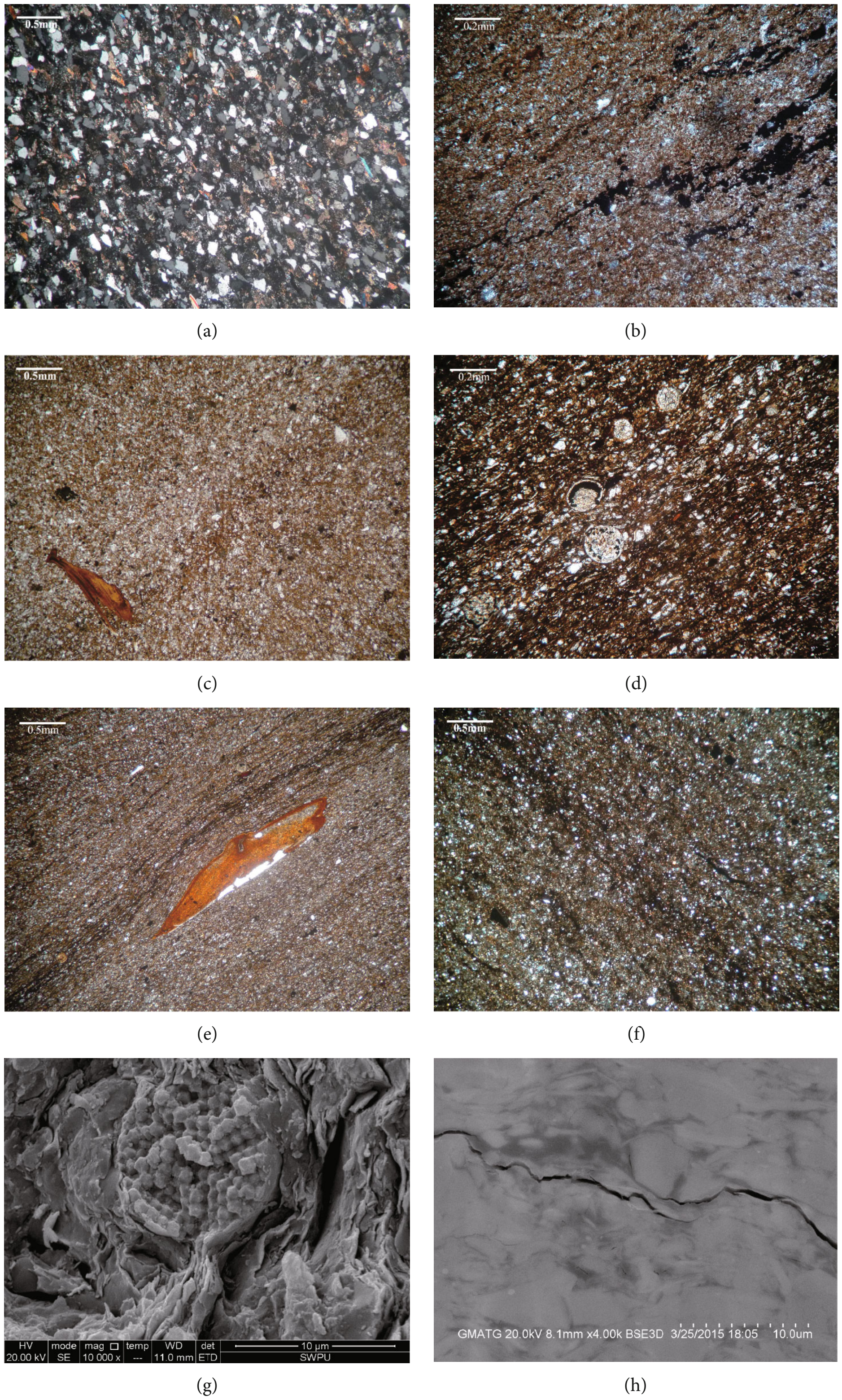

Figure 4: The photomicrographs of Chang 8 and 7^3 intervals in well DP1. (a) Fine-grained sandstone in the 6^{th} roundtrip. (b) Organic matter occurred along bedding in the 5^{th} roundtrip. (c–e) Biodetritus including phosphorus and spherical fragments in the 1^{st} to 5^{th} roundtrips. (f) Horizontal bedding in the 1^{st} roundtrip. (g) Framboidal pyrite with a size less than $7\,\mu$m in the Chang 7^3 interval. (h) Tiny cracks in the Chang 7^3 black shale. Note that (g–h) are obtained under scanning electron microscope.

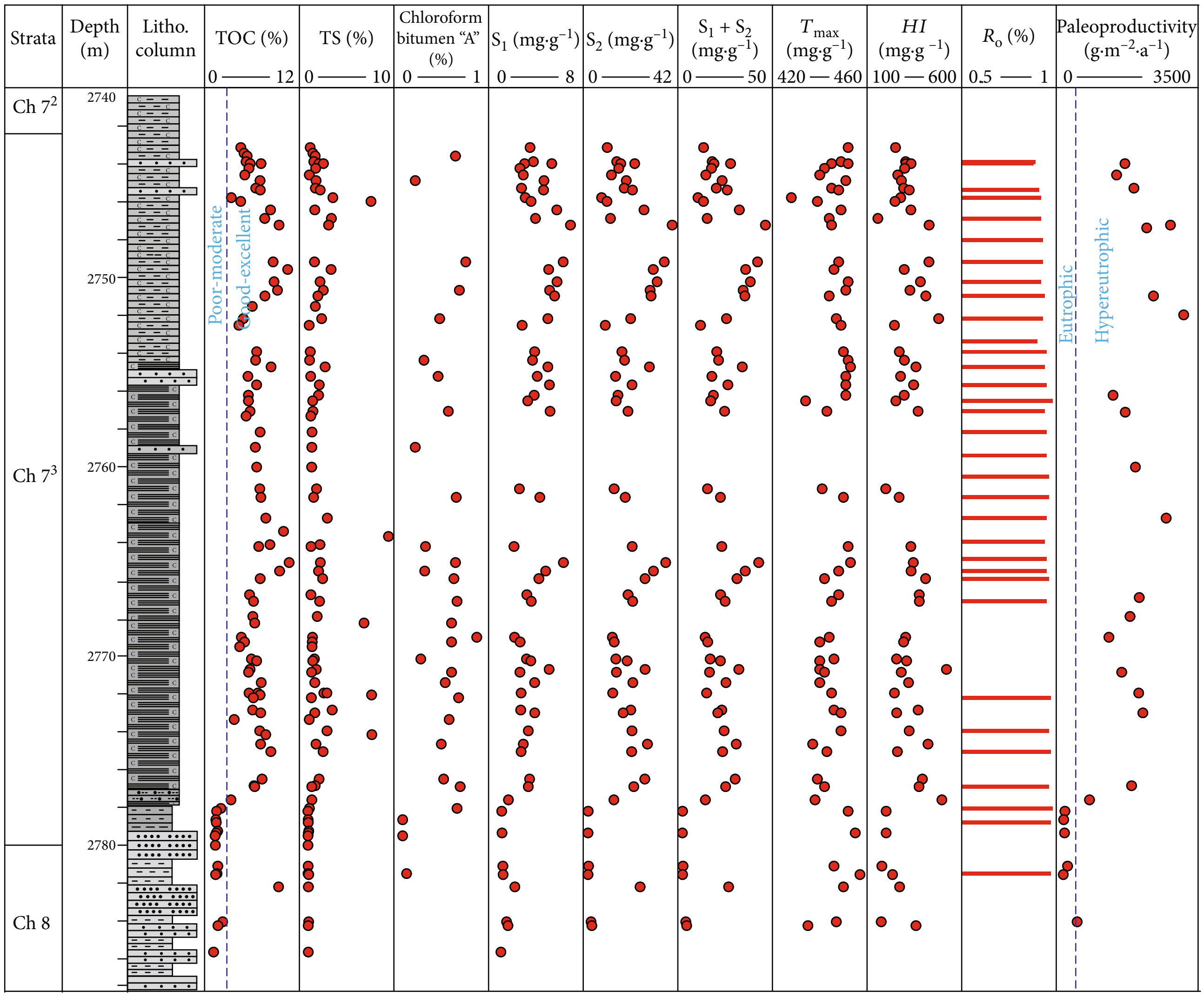

FIGURE 5: Geochemical log of well DP1 showing total organic carbon (TOC), total sulfur (TS), chloroform bitumen "A," vitrinite reflectance, Rock-Eval pyrolysis, and paleo-productivity. Note that the calculation formula of paleo-productivity is shown in Section 5.2.5.

variation in sedimentary facies demonstrates the rapid deepening process of lake water from the Chang 8 to early Chang 7 interval.

4.2. *Organic Geochemistry*

4.2.1. Organic Matter Content. The abundance of organic matter is the principal parameter for evaluating the source rock because it reflects the degree of enrichment of the residual organic matter in the source rock, is the material basis of oil and gas formation, and determines the hydrocarbon-generating potential of the source rock. The TOC, chloroform bitumen "A," and $S_1 + S_2$ values are widely used to comprehensively evaluate the organic matter abundance of source rocks. In this coring sample, the organic matter contents at different intervals show notable variation (Figure 5). The TOC values are lower in the Chang 8 member. The TOC values of all samples range from 0.22% to 1.47% ($n = 13$), with an average of 0.69% ($n = 14$), except for one sample that had a TOC value of more than 9%. The chloroform bitumen "A" and $S_1 + S_2$ values range from 0.01% to 0.06% and 0.55 mg/g to 26.37 mg/g, with an average of 0.03% ($n = 3$) and 7.35 mg/g ($n = 4$), respectively. The organic matter abundance in the Chang 8 member is consistent with their sedimentary environment dominated by the delta facies. The subsequent Chang7^3 sub-member shows a significant increase in organic matter abundance. Their TOC values range from 1.22% to 10.60%, with an average of 6.05% ($n = 73$). The chloroform bitumen "A," $S_1 + S_2$ values, and hydrogen index (HI) range from 0.17% to 0.95%, 1.46 mg/g to 46.21 mg/g, and 156.83 to 519.54, with an average of 0.56%, 22.76 mg/g, and 319.66, respectively (Figure 5; Tables 1–3).

4.2.2. Thermal Maturity. The thermal maturity of organic matter is an essential indicator of the quality of source rocks. The large-scale transformation of sedimentary organic matter to oil and gas requires an appropriate combination of temperature and time period. Organic matter generates a large amount of oil and gas on reaching thermal maturity.

Table 1: Rock-Eval pyrolysis data of Chang 7^3 and Chang 8 intervals from well DP1 in the western Ordos Basin.

Member	Depth (m)	T_{max} (°C)	S_1 (mg/g)	S_2 (mg/g)	$S_1 + S_2$ (mg/g)	HI index	OSI
Chang 7^3	2743.08	452.00	2.94	9.92	12.86	250.51	74.24
	2743.87	449.00	3.26	14.24	17.50	303.62	69.51
	2743.96	445.00	2.43	16.06	18.49	305.90	46.29
	2743.97	452.00	5.01	22.41	27.42	332.49	74.33
	2744.20	442.00	1.98	15.15	17.13	298.82	39.05
	2744.57	440.00	2.30	11.81	14.11	262.44	51.11
	2744.85	451.00	4.27	18.58	22.86	281.52	64.70
	2745.24	445.00	2.13	17.63	19.76	292.86	35.38
	2745.33	448.00	4.23	21.39	25.62	322.62	63.80
	2745.74	428.00	2.49	7.36	9.85	277.74	93.96
	2745.96	439.00	3.04	9.78	12.82	247.59	76.96
	2746.42	449.00	5.49	26.65	32.14	331.47	68.28
	2746.87	444.00	3.46	11.37	14.82	156.83	47.72
	2747.22	445.00	6.79	39.42	46.21	428.01	73.72
	2749.16	448.00	6.10	35.86	41.96	426.90	72.62
	2749.57	446.00	4.71	30.83	35.54	296.44	45.29
	2750.18	452.00	5.51	32.57	38.08	381.83	64.60
	2750.64	451.00	4.80	29.40	34.21	326.67	53.33
	2750.97	444.00	5.28	29.84	35.13	410.45	72.63
	2752.14	447.00	4.64	20.57	25.21	478.37	107.91
	2752.50	449.00	2.19	9.03	11.22	244.72	59.35
	2753.91	450.00	3.38	16.61	19.99	270.52	55.05
	2754.34	452.00	3.18	17.80	20.98	297.16	53.09
	2754.71	453.00	4.64	29.09	33.73	358.25	57.14
	2755.20	451.00	3.63	13.69	17.32	277.13	73.48
	2755.67	451.00	4.79	21.20	25.99	345.84	78.14
	2756.18	451.00	3.34	14.81	18.16	296.20	66.80
	2756.52	434.00	2.72	13.97	16.69	252.17	49.10
	2757.04	443.00	4.85	19.36	24.21	369.47	92.56
	2761.17	441.00	1.93	13.05	14.98	198.63	29.38
	2761.58	450.00	3.87	18.11	21.99	269.49	57.59
	2764.21	452.00	1.42	21.27	22.69	331.31	22.12
	2765.03	453.00	6.12	36.48	42.60	344.15	57.74
	2765.51	448.00	4.43	30.92	35.35	332.83	47.69
	2765.89	442.00	3.78	27.08	30.86	409.06	57.10
	2766.76	448.00	2.64	19.39	22.03	375.78	51.16
	2767.10	445.00	3.06	21.47	24.52	376.01	53.59
	2768.99	444.00	1.47	12.24	13.71	303.72	36.48
	2769.27	440.00	2.00	13.09	15.09	293.17	44.79
	2770.13	446.00	2.61	13.84	16.45	255.82	48.24
	2770.27	440.00	3.02	18.95	21.97	308.63	49.19
	2770.68	440.00	4.76	27.12	31.87	519.54	91.19
	2770.86	442.00	1.98	14.09	16.07	280.68	39.44
	2771.38	440.00	3.38	21.56	24.94	318.93	50.00
	2771.96	445.00	2.09	12.43	14.53	244.69	41.14
	2772.86	446.00	2.06	20.62	22.68	369.87	36.95
	2773.01	449.00	3.39	17.13	20.52	256.25	50.71
	2773.93	449.00	2.78	21.15	23.94	322.41	42.38

Table 1: Continued.

Member	Depth (m)	T_{max} (°C)	S_1 (mg/g)	S_2 (mg/g)	$S_1 + S_2$ (mg/g)	HI index	OSI
	2774.63	437.00	2.30	28.19	30.49	422.01	34.43
	2775.07	443.00	2.09	21.01	23.10	260.19	25.88
	2776.48	439.00	2.90	26.99	29.89	392.30	42.15
	2776.89	442.00	2.78	21.98	24.76	374.45	47.36
	2777.59	438.00	0.89	12.93	13.83	495.40	34.10
Chang 8	2778.18	452.00	0.25	1.26	1.51	200.96	39.87
	2779.34	455.00	0.28	1.18	1.46	200.68	47.62
	2781.10	446.00	0.36	1.43	1.79	177.97	48.30
	2781.57	457.00	0.38	1.18	1.55	234.83	103.07
	2782.18	450.00	1.50	24.87	26.37	271.80	53.83
	2784.03	447.00	0.71	2.57	3.29	174.83	107.91
	2784.25	435.00	0.84	2.92	3.76	358.28	2.95

Therefore, the maturity of organic matter is vital for evaluating the source rocks [27]. R_o and T_{max} are common indicators that reflect the degree of thermal evolution of organic matter. The core samples in this study exhibit relatively uniform thermal maturity, with R_o values ranging from 0.88% to 0.98%, with an average of 0.94% ($n = 33$; Figure 5; Table 4), indicating that all samples are in the stage of the oil generation window. The T_{max} value ranges from 428 °C to 457 °C, with an average of 446 °C ($n = 60$), indicating the maturation stage (Figure 5). The R_o and T_{max} results are relatively consistent, indicating the accuracy of the test data.

4.2.3. Organic Material Type. The type of organic matter in the source rocks affects the hydrocarbon generation potential of the source rocks and the characteristics of hydrocarbon products. The organic macerals and Rock-Eval pyrolysis parameters are often used to characterize organic matter types. Because of the influence of terrestrial organic matter input, lacustrine source rocks are substantially more heterogeneous than marine source rocks. The organic maceral components of the source rocks formed in different environments are significantly different. Most of the organic matter in the source rocks is composed of sapropelite, vitrinite, exinite, and inertinite. The relatively proportional assemblage of these four components reflects the source of the organic matter in the lake. The change in organic macerals is negligible in all the 33 samples in this study, indicating that the sources of organic matter are similar. Figure 6 shows that the organic matter type of the Chang 7^3 sub-member of well DP1 is mainly type II_2. The Rock-Eval pyrolysis data can also be used to determine the type of organic matter. According to Figure 7 [28], most of the samples in well DP1 are type II, and small amounts belong to type I. Thus, the Rock-Eval pyrolysis results are slightly different from those of the organic maceral components. However, the primary analysis result is type II kerogen, suggesting abundant terrigenous organic matter input into the study area.

4.3. Element Geochemistry. Fifteen black shale samples from the middle part of the Chang 7^3 sub-member in well DP1 were undertaken for whole-rock element analysis. As shown in Table 5, all the major and trace elements of the samples show steady variations within a narrow range. The redox index Ce anomaly (Ce/Ce*) ranges from 0.82 to 1.03, with an average of 0.9. The U/Th and Fe_T/Al ratio values range from 0.09 to 0.15 and 0.30 to 0.53, with an average of 0.11 and 0.39, respectively. The chemical index of alteration (CIA) ranges from 67.71 to 83.24, with an average of 74.31. The SiO_2 and $Al_2O_3 + K_2O + Na_2O$ ratios range from 61.41 to 68.04 and 21.74 to 24.81, with an average of 66.91 and 23.10, respectively. The hydrothermal index (Fe + Mn) /Ti and Al/(Al + Fe + Mn) ratio values range from 6.86 to 11.93 and 0.65 to 0.77, with an average of 8.49 and 0.72, respectively (Figure 8). The TS values range from 0.14% to 9.93%, with an average of 1.51%. The TS/TOC and Sr/Ba ratio values range from 0.03 to 1.86 and 0.45 to 1.35, with an average of 0.25 and 0.63, respectively.

5. Discussion

5.1. Source Rock Evaluation. The black shales of the Chang 7 member in the Ordos Basin are generally characterized by a wide distribution area, large thickness, abundant organic matter, and suitable organic matter type and thermal maturity. Thus, it is regarded as the most significant oil and gas source for the entire Mesozoic oil reservoir [7, 24]. The characteristics of source rocks vary in different regions due to the frequent changes in sedimentary facies in continental lacustrine basins. Thus, it is inaccurate to determine the regional "sweet spot" of oil and gas exploration. Previous studies on the Chang 7 member have been focused on the southern part of the basin. Fu et al. [11] discovered the largest shale oil reservoir in China, the Qingcheng Oilfield, which greatly promoted an increase in oil and gas production and resource reserves in the Ordos Basin. However, few study on the Chang 7^3 sub-member of the Tianhuan Depression is available. In addition, the Chang 7^3 sub-member is gaining attention as the largest period of late Triassic lake transgression because of the black rock series with the largest abundance of organic matter and the widest area among the Chang 7 sub-members.

Table 2: The TOC and TS content of Chang 7^3 and Chang 8 intervals from well DP1 in the western Ordos Basin.

Member	Depth (m)	TOC (%)	TS (%)	TS/TOC
Chang 7^3	2743.08	3.96	0.26	0.07
	2743.42	4.41	0.57	0.13
	2743.57	4.83	0.84	0.17
	2743.87	4.69	0.68	0.14
	2743.96	5.25	1.29	0.25
	2743.97	6.74	1.80	0.27
	2744.20	5.07	0.90	0.18
	2744.57	4.50	0.16	0.04
	2744.85	6.60	0.94	0.14
	2745.24	6.02	0.87	0.15
	2745.33	6.63	1.43	0.22
	2745.74	2.65	2.90	1.09
	2745.96	3.95	7.33	1.86
	2746.42	8.04	0.80	0.10
	2746.87	7.25	2.73	0.38
	2747.22	9.21	2.40	0.26
	2749.16	8.40	0.76	0.09
	2749.57	10.40	2.69	0.26
	2750.18	8.53	1.41	0.17
	2750.64	9.00	1.79	0.20
	2750.97	7.27	1.15	0.16
	2752.14	4.30	1.59	0.37
	2752.50	3.69	0.14	0.04
	2753.91	6.14	0.27	0.04
	2754.34	5.99	0.19	0.03
	2754.71	8.12	2.00	0.25
	2755.2	4.94	0.32	0.06
	2755.67	6.13	1.32	0.22
	2756.18	5.00	1.23	0.25
	2756.52	5.01	0.55	0.11
	2751.52	5.54	0.86	0.15
	2757.04	5.24	0.58	0.11
	2757.31	4.69	0.33	0.07
	2758.16	6.61	0.48	0.07
	2758.93	5.96	0.45	0.08
	2759.98	6.14	0.43	0.07
	2761.17	6.57	1.00	0.15
	2761.58	6.72	0.66	0.10
	2762.68	7.40	2.25	0.30
	2763.42	9.83	9.93	1.01
	2764.09	7.96	1.40	0.18
	2764.21	6.42	0.35	0.05
	2765.03	10.60	1.44	0.14
	2765.51	9.29	1.23	0.13
	2765.89	6.62	1.71	0.26
	2766.76	5.16	0.34	0.07
	2767.1	5.71	1.35	0.24
	2767.92	5.61	1.08	0.19
	2768.24	5.87	6.52	1.11
	2768.99	4.03	0.53	0.13
	2769.27	4.47	0.50	0.11
	2769.50	3.80	0.48	0.13
	2770.13	5.41	0.75	0.14
	2770.27	6.14	0.56	0.09
	2770.68	5.22	0.97	0.19
	2770.86	5.02	0.42	0.08
	2771.38	6.76	0.80	0.12
	2771.96	6.30	1.85	0.29
	2772.03	6.61	7.40	1.12
	2772.20	5.68	0.40	0.07
	2771.96	5.08	2.21	0.44
	2772.86	5.58	2.82	0.51
	2773.01	6.69	0.80	0.12
	2773.37	3.05	0.15	0.05
	2773.93	6.56	2.22	0.34
	2774.63	6.68	0.93	0.14
	2775.07	8.08	1.76	0.22
	2774.15	7.39	7.43	1.01
	2776.48	6.88	1.30	0.19
	2776.83	5.77	0.84	0.15
	2776.89	5.87	0.44	0.07
	2777.59	2.61	0.45	0.17
	2778.06	1.22	0.17	0.14
Chang 8	2778.18	0.63	0.00	0.00
	2778.67	0.53	0.02	0.03
	2778.78	0.59	0.03	0.05
	2779.24	0.78	0.10	0.13
	2779.34	0.59	0.04	0.07
	2779.48	0.43	0.01	0.02
	2780.01	0.46	0.01	0.01
	2781.1	0.80	0.02	0.02
	2781.52	0.69	0.01	0.01
	2781.57	0.50	0.09	0.18
	2782.18	9.15	0.05	0.01
	2784.03	1.47	0.08	0.06
	2784.25	0.82	0.03	0.04
	2785.63	0.22	0.04	0.16

In the well DP1, the Chang 7^3 sub-member has an average TOC of 6.05%, an average chloroform bitumen "A" of 0.56%, and a hydrocarbon generation potential of 22.76 mg/g. It is classified as a good-excellent source rock based on the S_2-TOC diagram ([29]; Figure 9). Several studies on the Chang 7^3 sub-member in the Tianhuan Depression have reported similar characteristics of TOC to those in this study. For example, Huang [30] reported the average values of the TOC, chloroform bitumen "A," and $S_1 + S_2$ to be 5.40%, 0.84%, and 21.67 mg/g, respectively, in the Chang

Table 3: Chloroform bitumen "A" content of Chang 7^3 and Chang 8 intervals from well DP1 in the western Ordos Basin.

Member	Depth (m)	Chloroform bitumen "A" (%)
	2743.57	0.68
	2744.85	0.17
	2749.16	0.81
	2750.64	0.73
	2752.14	0.48
	2754.34	0.28
	2755.20	0.46
	2757.04	0.59
	2758.93	0.17
	2761.58	0.69
	2764.21	0.30
	2765.03	0.68
	2765.51	0.29
Chang 7^3	2765.89	0.66
	2767.10	0.70
	2768.24	0.63
	2768.99	0.95
	2769.27	0.63
	2770.13	0.24
	2770.86	0.63
	2771.38	0.55
	2772.20	0.72
	2773.37	0.60
	2774.63	0.50
	2776.48	0.53
	2776.89	0.74
	2778.06	0.70
	2778.67	0.01
Chang 8	2779.48	0.01
	2781.52	0.06

Table 4: Vitrinite reflectance (R_o) of Chang 7^3 and Chang 8 intervals from well DP1 in the western Ordos Basin.

Member	Depth (m)	R_o (%)	Standard deviation	Number
	2743.87	0.89	0.02	23
	2743.97	0.88	0.01	21
	2745.33	0.91	0.02	16
	2745.74	0.92	0.02	31
	2746.87	0.92	0.01	22
	2748.00	0.93	0.02	11
	2749.16	0.93	0.02	23
	2750.18	0.92	0.01	24
	2750.97	0.94	0.02	26
	2752.14	0.93	0.02	20
	2753.35	0.90	0.02	21
	2753.91	0.95	0.03	25
	2754.71	0.94	0.01	26
	2755.67	0.95	0.03	11
	2756.52	0.98	0.01	26
Chang 7^3	2757.04	0.94	0.02	23
	2758.16	0.95	0.02	24
	2759.42	0.95	0.01	28
	2760.48	0.96	0.02	22
	2761.58	0.96	0.02	16
	2762.68	0.95	0.02	14
	2763.93	0.94	0.01	16
	2764.87	0.95	0.03	25
	2765.51	0.95	0.02	12
	2765.89	0.96	0.01	22
	2767.10	0.95	0.02	23
	2772.20	0.97	0.02	24
	2773.93	0.96	0.02	21
	2775.07	0.97	0.02	23
	2776.89	0.96	0.02	24
	2778.06	0.98	0.01	20
Chang 8	2778.78	0.97	0.01	16
	2781.52	0.97	0.02	22

7^3 sub-member from the well Feng75 of the adjacent area. In the northern Jiyuan area of the Tianhuan Depression, the average TOC of Chang 7 member was 3.68% [31]. In comparison, the TOC value is higher in other areas, particularly in the southern region of the Ordos Basin. For instance, Ji et al. [32] reported that in the well YK1 of the south Ordos Basin, the TOC and $S_1 + S_2$ values of Chang 7^3 shale range from 0.5% to 29.91% and 0.1 mg/g to 146.84 mg/g, with an average of 10.52% ($n = 44$) and 53.17 mg/g ($n = 44$), respectively. In the same drilling, the average values of TOC and $S_1 + S_2$ can be 18.16% and 89.92 mg/g, respectively [33], which is significantly higher than the values obtained in this study. Based on a comprehensive analysis, in the center of the Ordos Basin, the average TOC of Chang 7^3 sub-member is 13.8%, and the maximum is up to 30–40% [24, 34]. These results demonstrate that the TOC of the Chang7^3 sub-member is relatively high across the Ordos Basin and that the organic matter content is not homogeneous in the plane.

The thermal evolution degree of organic matter from the well DP1 is at the peak of oil generation, and the type of organic matter tends to generate oil with a thickness of up to 40 m. Although there are certain differences in the plane distribution due to the influence of sedimentary facies and geological tectonics, the Chang 7^3 sub-member in the Mahuangshan area of the Tianhuan Depression is a high-quality source rock according to the geochemical evaluation by using the method of continental source rocks developed by the Standardization Committee of Petroleum Geological Exploration [35]. The hydrocarbon generation potential of the Chang 7^3 organic-rich shales in the central area of the lake basin mainly ranges from 30 to 50 mg/g (up to 150 mg/g), displaying excellent hydrocarbon generation and expulsion ability (e.g., [15]), which is significantly

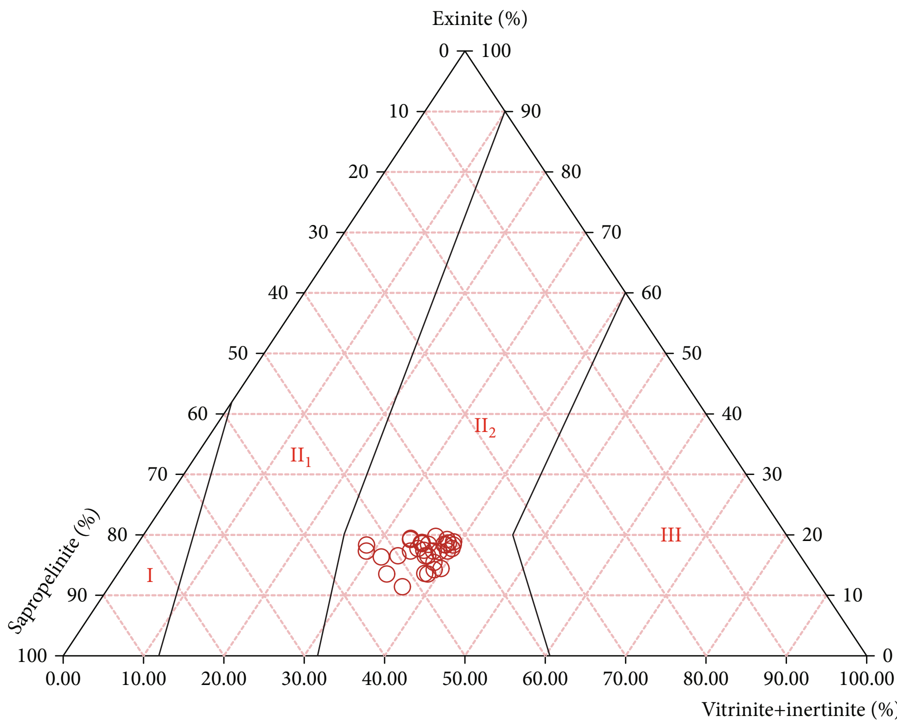

Figure 6: Ternary diagrams of organic maceral components in well DP1.

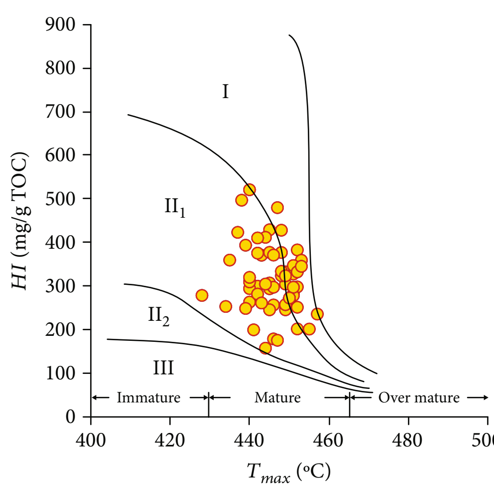

Figure 7: Chart of HI versus the Rock-Eval pyrolysis temperature of the maximum [28] for well DP1 in the western Ordos Basin.

higher than that in well DP1. The results of this study suggest that the source rock of the Chang 7^3 interval shows good–excellent overall oil and gas exploration potential. The T_{max} value of the Chang 7^3 sub-member in another well drilling (Feng75) sample from the Tianhuan Depression ranges from 424 °C to 450 °C, which is similar to the results of this study [30]. Reports from other regions have also shown that the source rocks of the Chang 7^3 sub-member are in the maturation stage [34]. The T_{max} value ranges from 428 °C to 451 °C, with an average of 439 °C ($n = 44$) in YK-1 located at the southern margin of the Ordos Basin [32]. However, the degree of thermal evolution of the Chang 7 member of the basin also has certain zoning. Cui et al. [36] reported a R_o value of more than 0.8% in northern Shaanxi, eastern Gansu, and the southeast of the Ordos Basin and less than 0.8% in other areas. The thermal anomaly in the Wuqi–Qingyang–Fuxian area of the southern Ordos Basin might be attributed to the differences in maturity of organic matter.

The quality of the source rocks in the Chang 7 member of the Ordos Basin is generally related to the distribution of the sedimentary facies. The Mahuangshan area was located in the northwestern margin of the lake basin during the Late Triassic Chang 7 period. Thus, the area was affected by the surrounding terrigenous input, resulting in regionally specific organic matter abundance and type. For example, the higher $C_{19}TT/C_{23}TT$ and $C_{24}TeT/C_{26}TT$ ratios of biomarkers in the adjacent well Feng75 in the Tianhuan Depression suggest that the abundance of terrigenous organic matter in the Chang 7^3 sub-member is significantly higher than that in the Chang 7^1 and Chang 7^2 sub-members [23]. In the well DP1 area, more terrigenous detrital components were also observed in the thin section of the Chang 7^3 sub-member, which indicates that the study area might have been subjected to a relatively strong input of terrigenous organic matter. Nevertheless, previous studies have shown that the entire Ordos Basin was deposited mainly in semi-deep and deep lake environments during the Chang 7 period. Therefore, the organic macerals of high-quality source rocks in the Chang 7 members are principally sapropelite [16, 37–39], with no or rarely terrigenous inputs [34]. In the well YK1 of the southern Ordos Basin, the organic matter types of Chang 7^3 sub-member are mainly type I and type II_1, and the types II_2 and III account for only 5% and 2.5%, respectively [32]. In summary, the organic matter

Table 5: Element geochemical data for of Chang 7^3 interval from well DP1 in the western Ordos Basin.

Member	Depth (m)	U/Th	Fe_T/Al	Ce*	Fe/Mn	Mn/Ti	SiO_2 (%)	$Al_2O_3+K_2O+Na_2O$	CIA	(Fe + Mn)/Ti	Al/(Al + Fe + Mn)	Sr/Ba
Chang 7^3	2764.89	0.11	0.37	0.97	52.94	0.15	66.94	23.20	70.25	8.08	0.73	0.45
	2765.31	0.15	0.50	0.97	81.35	0.13	66.72	21.74	69.23	10.67	0.66	0.52
	2766.89	0.12	0.37	0.87	66.99	0.12	66.76	24.09	68.64	8.39	0.73	0.56
	2767.43	0.10	0.30	0.93	56.59	0.12	66.59	24.81	71.66	6.95	0.77	0.67
	2767.92	0.11	0.36	0.92	56.44	0.14	67.74	22.96	68.92	8.04	0.73	0.59
	2768.07	0.11	0.39	0.86	57.31	0.15	68.04	22.40	67.71	8.58	0.72	0.59
	2768.61	0.10	0.42	0.83	72.94	0.12	67.39	22.29	69.69	8.70	0.70	0.60
	2768.72	0.12	0.35	0.84	80.08	0.10	66.41	24.12	75.22	7.80	0.74	0.70
	2769.5	0.11	0.37	0.87	57.99	0.14	67.39	23.55	70.60	7.98	0.73	0.56
	2770.13	0.12	0.32	0.82	57.11	0.12	67.72	23.88	75.66	6.86	0.76	0.54
	2770.43	0.09	0.38	0.90	39.33	0.21	67.82	22.32	78.24	8.41	0.72	0.63
	2770.86	0.11	0.32	0.86	43.20	0.16	67.99	23.64	81.70	7.27	0.75	0.54
	2771.96	0.11	0.43	0.82	78.35	0.12	66.72	22.98	83.24	9.45	0.70	0.51
	2772.52	0.14	0.53	1.03	46.86	0.25	61.41	21.93	82.83	11.93	0.65	1.35
	2773.01	0.11	0.40	0.95	54.37	0.15	67.99	22.57	81.00	8.24	0.71	0.60

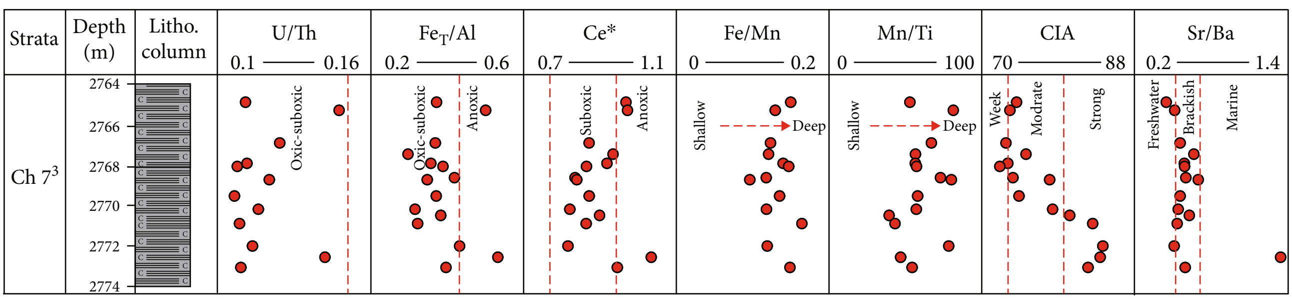

Figure 8: Element geochemical column of Chang 7^3 black shale in well DP1 showing paleoenvironment, paleowater depth, chemical weathering, and paleosalinity. Note that the dashed lines indicate the thresholds for these geochemical proxies.

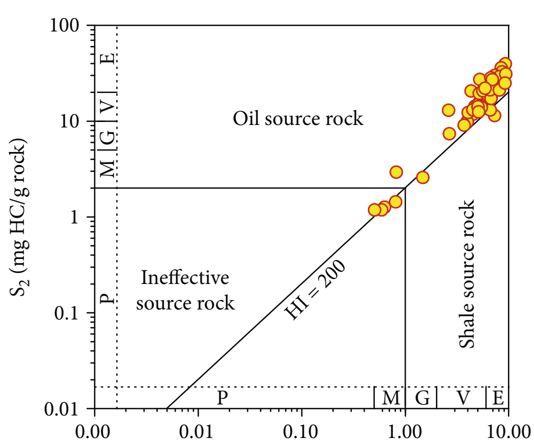

Figure 9: Discrimination diagram of S_2 versus total organic carbon (TOC) for source rock evaluation [29]. Note that the P, M, G, V, and E represent the poor, moderate, good, very good, and excellent, respectively.

types of the Chang 7^3 sub-member in different regions vary owing to the effect of sedimentary facies and provenance distribution, and the primary types of organic matter are type I and type II_1. In contrast, organic matter types II_2 and III in some regions might be affected by the neighboring terrigenous input (e.g., [18, 34]).

Furthermore, heavy mineral analysis demonstrates that the entire Chang 7 member of the Ordos Basin has five main provenance areas, while the Yanchi-Dingbian area in the northwest is one of the provenances in the lake basin [21, 40]. This area is characterized by “high garnet content, low zircon content, relatively low titanomorphite content,” “relatively higher feldspar content and relatively lower quartz content,” and “relatively high metamorphic lithic fragment content.” Therefore, Wang et al. [41] and Zhang et al. [40] reported that the provenance might have been supplied by the Bayanhot area of the Alashan ancient block in the northwest, resulting in the development of a meandering river delta front environment in certain areas [42]. Consequently, the Mahuangshan area was affected by terrigenous input (such as massive mudstone and detrital grains) to a greater extent than the semi-deep lake–deep lake areas in the southwestern and southeastern basins, causing a highly proportional humic component and a relatively low TOC value in well DP1. This also explains why the Chang 7^3 sub-member source rock from the Mahuangshan area is inferior to that of the area without an undisturbed deep-lake environment [43].

5.2. Sedimentary Environment

5.2.1. Redox Condition. The redox state of the bottom water is the main factor for the effective preservation of organic matter, which controls the development characteristics of high-quality source rocks in the plane. Bimetal ratio proxies and rare earth elements in fine-grained rocks are widely employed to distinguish the redox conditions of sedimentary water columns, such as U/Th, Fe_T/Al, and Ce/Ce*. Jones and Manning [44] reported that U/Th values of less than 0.75 and greater than 1.75 indicate oxic and anoxic environments, respectively. The ratio of Fe_T/Al in the upper crust is 0.44 [45], whereas the Fe_T/Al ratios of ancient sediments are greater than this threshold value, showing anoxic conditions [46]. The Ce anomaly ($Ce/Ce^* = Ce_N/(La_N \times Pr_N)(1/2)$) in ancient sediments is another useful geochemical indicator of the redox conditions. Shields and Stille [47] reported that Ce/Ce* is less than 0.5 under oxic condition, 0.6–0.9 under suboxic condition and 0.9–1.0 or even higher than 1.0 under anoxic condition. In this study (Figure 8), the U/Th ratio in the Chang 7^3 sub-member indicates oxic bottom water conditions, while the Fe_T/Al ratios show an oxic with episodically suboxic setting. Meanwhile, the Ce/Ce* values were all greater than 0.5, and one sample reached 1.03, indicating an anoxic environment during the Chang 7^3 period. Despite the contradictions among geochemical indicators, Algeo and Liu [48] proposed that the bimetal ratio proxy is commonly affected by terrigenous input and diagenesis and hence may not be a reliable redox indicator. In contrast, rare earth elements are rarely affected during the migration process. Therefore, Ce/Ce* may have improved the efficiency of the redox state in bottom water. Additionally, this study also found that most shales exhibited remarkable horizontal bedding, framboidal pyrite with a small size (Figure 4(g)), pyrite nodules (Figure 3(d)), and high content of TS (up to 9.93%). Consequently, it is considered that the Chang 7^3 sub-member from well DP1 might have been predominantly deposited in the relatively suboxic–anoxic bottom water accompanied by transient and repeated oxic state fluctuations.

The different paleowater depths may correspond to different redox status in ancient lake systems. Li et al. [49] and Zheng et al. [50] suggested that Fe/Mn and Mn/Ti can be applied to determine the paleowater depth based on the chemical differences in Fe, Ti, and Mn. As shown in Figure 8 and Table 5, the Fe/Mn ratios in this study are all less than 100, and the Mn/Ti ratios range from 0.1 to 0.3, indicating a relatively deep lake environment during the deposition of Chang 7^3 interval. This is consistent with the results interpreted from sedimentological observations. As the maximum period of the lake level, the Chang 7^3 sub-member through the Ordos Basin was mainly deposited in deep lakes, resulting in oxygen-depleted lake bottom water [14]. However, since the Mahuangshan area is located at the margin of the provenance region, it might have been impacted by the transient delta front detrital input, thus appearing as an oxic-suboxic environment in partial layers. For instance, during the Chang 7^3 interval, the redox state of the bottom water near the study area (wells Y56 and Feng75) was weakly oxic-suboxic, rather than strongly anoxic [16, 23, 30, 51]. In contrast, the southeast and southwest regions of the lake basin usually presented a redox state of strong reduction or even euxinic, indicating that the lake water was stratified [52–55]. In this scenario, the sedimentary organic matter would be well preserved, causing the TOC content in the deep lake area to remarkably increase compared with that in the Mahuangshan area.

5.2.2. Paleoclimate. Paleoclimate dominates organic matter production and accumulation by affecting surface sedimentary processes and terrigenous inputs [15]. The relative content and ratio of certain elements in sedimentary rocks, such as the CIA index and the discrimination diagram of SiO_2 vs $Al_2O_3 + K_2O + Na_2O$, can be used to reconstruct the coeval paleoclimate [56]. According to Nesbitt and Young [57], CIA values of 100–80, 80–70, and 70–50 reflect strong, moderate, and weak chemical weathering intensities in the provenance area, respectively. The detailed calculation method for CIA has been described by Li et al. [15]. In this study, the CIA value ranges from 67.71 to 83.24 (Figure 8), with an average of 74.31, indicating a moderate to strong weathering intensity in the source areas. Meanwhile, the discrimination diagram of SiO_2 vs $Al_2O_3 + K_2O + Na_2O$ suggests that the paleoclimate was under warm and humid conditions (Figure 10).

Previous studies on the paleoclimate of the entire Late Triassic in the Ordos Basin achieved a relatively consistent conclusion. Li et al. [15] examined the geochemical data of well JH-4 in the southwest basin and found that the average C-value of the Chang 7 member is 0.8 and the CIA value ranges from 71.30 to 81.97, with an average of 75.48. It is considered that the entire Chang 7 member was deposited under a warm humid paleoclimate, wherein the Chang 7^3 sub-member was formed in the most humid conditions with moderate weathering intensity. This inference is also supported by studies investigating wells YQ-1 and YK-1 in the southeastern basin [33, 54], southern basin [58], and the entire basin [14]. The geochemical results of Al_2O_3/MgO, Sr/Cu, and Rb/Sr from well Feng75 in the same study area indicate that the paleoclimate of the Chang 7^3 member was in warm and humid conditions and the paleotemperature gradually increased [30]. Additionally, Zhu et al. [59] claimed that the North China plate was located at approximately 25°N latitude during the Late Triassic period on the basis of paleomagnetic evidence, which is in line with its paleogeographic position. Based on these geochemical facts, the entire Ordos Basin exhibited a similar paleoclimate during the Chang 7^3 period, which was warm and humid with moderate continental weathering intensity, providing favorable climatic conditions for the flourishing of lacustrine phytoplankton in the surface water and the import of terrestrial organic matter. The higher proportions of terrigenous exinite and inertinite in this study also appear to support this conclusion (Figure 6).

5.2.3. Volcanic and Hydrothermal Activities. Previous studies from the Ordos Basin discovered that tuff layers with a large cumulative thickness developed in the entire Chang 7

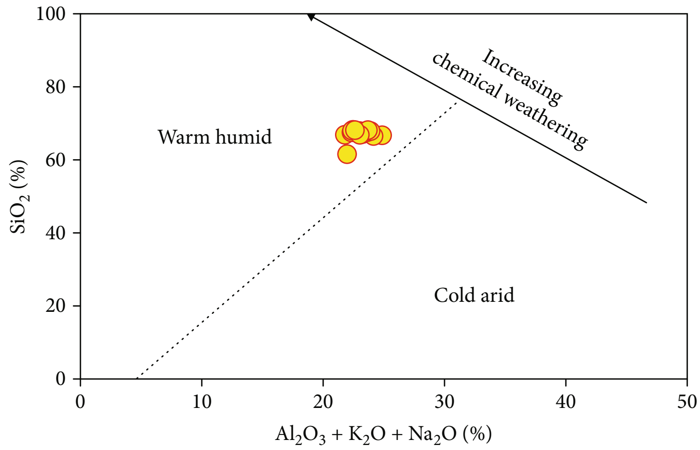

FIGURE 10: Discrimination diagram of SiO_2 versus ($Al_2O_3 + K_2O + Na_2O$) for paleoclimate [56] in the Chang 7^3 black shale.

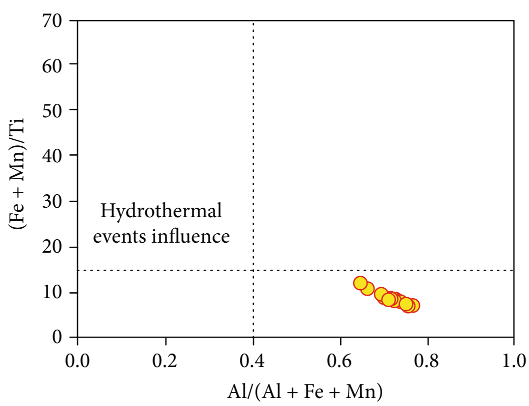

FIGURE 11: Discrimination diagram of (Fe + Mn)/Ti versus Al/(Al + Fe + Mn) for the influence of hydrothermal activity [60] in the Chang 7^3 black shale.

member, implying that there was a certain genetic relationship between the deposition of organic-rich rocks and contemporaneous volcanic activities [7], and the eruption intensity dominated the primary productivity [17]. Volcanic and hydrothermal activities contribute large amount of Fe and Mn elements; therefore, (Fe + Mn)/Ti and Al/(Al + Fe + Mn) are employed to illustrate whether sediments are affected by volcanic and hydrothermal activities [60]. Ji et al. [32] reported that the (Fe + Mn)/Ti and Al/(Al + Fe + Mn) values of most samples in the Chang 7^2 and Chang 7^3 sub-members from well YK1 in the southern margin of the basin were significantly greater than 15 and less than 0.4, respectively, suggesting that these wells had been seriously subjected to hydrothermal fluid. In contrast, the geochemical proxies (Fe + Mn)/Ti and Al/(Al + Fe + Mn) suggest that there is no obvious effect of volcanism and hydrothermal activities across the area of well DP1 (Figure 11). These volcanic activities are commonly thought to originate from intensive felsic volcanism in the southwestern Ordos Basin, induced by the collision of the Yangtze and North China plates during the Late Triassic period [61]. The Mahuangshan area is far from the volcanic source than the southern Ordos Basin, which might have contributed to the lower influence of volcanic ash on this area. However, volcanic activity frequently brings abundant nutrient elements, improves surface primary productivity, and enhances the salinity of the water column [7, 30], which is conducive to the production and preservation of organic matter [62]. Zheng [63] discovered that thermophilic organisms (i.e., collophanite-like algae and round-shaped algae) are contained in the Chang 7^3 sub-member. The degree of development of these organisms is most closely related to the hydrothermal exhalative rock, which can provide a significant amount of heat, further explaining that the surface primary productivity is related to these activities inside the earth. However, organic-rich matter deposition can occur without the effect of volcanism, indicating that volcanic and related hydrothermal activities might not be the primary controlling factor for the extreme organic matter enrichment in the Chang 7^3 sub-member.

5.2.4. Paleosalinity. The geochemical proxies Sr/Ba (fresh water, brackish water, and sea water) and TS/TOC (fresh water and non-fresh water) are used as effective tools to determine the paleosalinity of sedimentary water. The Sr/Ba ratio of greater than 0.5 and the TS/TOC ratio of greater than 0.1 indicate that the water column is a brackish or normal marine environment. However, when these ratios are less than 0.2 and 0.1, respectively, they imply fresh water conditions [64]. As shown in Figures 8 and 12, most of the samples fall into the brackish–marine environment, indicating relatively high paleosalinity during the sedimentary period of the Chang 7^3 sub-member at the study site. Based on geochemical data from the adjacent well Feng75, a distinct increase in salinity occurred in the middle part of the Chang 7^3 sub-member [30]. Such paleosalinity features in the Mahuangshan area show that the study area should have similar paleohydrological conditions.

Previous studies have suggested that the Chang 7^3 sub-member should be mainly deposited in fresh or weakly brackish water environments [16, 43], although some areas show brackish water even in marine environments [15, 54, 65]. Liu et al. [7] hypothesized that the view of brackish-marine water might be due to the influence of a large

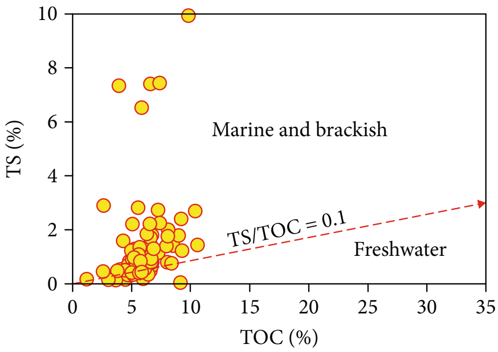

Figure 12: Discrimination diagram of total sulfur (TS) versus total organic carbon (TOC) [64] for the paleosalinity of Chang 7^3 interval.

number of external sulfate inputs (such as volcanic and hydrothermal activities) during the deposition of the Chang 7^3 sub-member, resulting in an increase in its TS content. A similar inference was reported by Huang [30]. However, the Sr/Ba ratio in this study also indicates a normal marine environment, and the study area was not seriously affected by volcanic and hydrothermal activities. Therefore, the explanation raised by Liu et al. [7] cannot demonstrate that the study area has the characteristics of high-salinity water. Based on the comprehensive analysis of regional provenance, this study believes that the local salinization of deep water in the Chang 7^3 sub-member of the Mahuangshan area might be related to the invasion of ambient seawater or water stratification. This situation also appears in wells JH4 and YW1 in the southern part of the basin [15, 66]. In addition, the study of lacustrine sediments from the Songliao Basin, Bohai Bay Basin, and Qaidam Basin revealed that salinization of deep lake water easily leads to water stratification, thus promoting the preservation of organic matter and facilitating the formation of high-quality source rocks [67, 68]. Consequently, high-salinity lake water can contribute to the enrichment of organic matter in the Chang 7^3 sub-member.

5.2.5. Paleo-Productivity. Primary productivity in surface lake water is a major source of organic matter. Therefore, it is one of the most critical factors for controlling organic matter enrichment. Currently, the paleo-productivity proxies (Ba_{bio} and P_{bio}; [55]) of the black rock series in the Chang 7^3 sub-member are mostly qualitative descriptions [15], which cannot be well compared at the basin-scale. Müller and Suess [69] provided the following equation to quantitatively characterize paleo-productivity using organic carbon:

$$\mathrm{R} = \mathrm{C} \times p_s \times \frac{1-\varphi}{0.0030 \times \mathrm{S}^{0.30}}. \tag{1}$$

R, C, p_s, φ, and S represent paleo-productivity (g/m^2·a), organic carbon content (%), porosity (g/cm^3), sediment density (%), and sedimentation rate (cm/1000a), respectively.

However, this formula is mainly applicable to marine areas without the influence of terrestrial organic matter. Therefore, this study corrected the formula according to the specific situation of this study, by multiplying TOC by the proportion of lacustrine organic matter. The coefficient is based on the ratio of $(C_{15} + C_{17} + C_{19})/(C_{27} + C_{29} + C_{31})$ in the Chang 7 member to represent the ratio of aquatic to terrestrial organisms in the water column. Wang [16] reported this ratio to be 0.731 for the Chang 7^3 sub-member. In addition, some measured data were used in this study because well Y56 is closer to the study area. For instance, the porosity was obtained from the measured value of 0.42 for the Chang 7^3 sub-member [16]. The sedimentation rate was obtained from the value of the Chang 7^3 sub-member in well Y56, calculated by Chen et al. [19] using cyclostratigraphy, with an average value of 1.3. The measured rock density and original TOC values in this study are listed in Table 6. According to the above equation, the paleo-productivity was distributed between 172.16 and 3141.62 g/(m^2·a), with an average value of 1543.91 g/(m^2·a) (Figure 5). The lowermost interval of Chang 7^3 had a smaller primary productivity (ca. 259.94 g/(m^2·a)). The primary productivity increased sharply with the increase in TOC and remained between 1000 and 3000 g/(m^2·a), displaying an extremely high paleo-productivity.

Kelts [70] proposed a scheme for the classification of nutrient types in modern lakes, which classified modern lakes into oligotrophic (100–180 g/(m^2·a)), mesotrophic (200–310 g/(m^2·a)), eutrophic (350–680 g/(m^2·a)), and hypereutrophic (1000–6000 g/(m^2·a)). The paleo-productivity of the Chang 7^3 sub-member in this study is equal to that of hypereutrophic lakes, corresponding to the Turkana Lake (Kenya) to Aranguadi Lake (Ethiopia). Similar results were obtained for well Y56 [16]. However, in terms of evolutionary trend, the paleo-productivity of well DP1 started from the mesotrophic lake type in the Chang 8 interval, rose sharply by lake transgression in the early Chang 7^3 interval, and subsequently remained steady in the hypereutrophic lake type until the end of the Chang 7^3 interval. In contrast, the paleo-productivity of the nearby well Y56 gradually declined in the late Chang 7^3 period, but remained within the range of hypereutrophic lake types.

Because the bottom water in the study area is dominantly suboxic-anoxic, biogenic elements such as P and Ba are easily released into the water by redox fluctuations. Thus, their content is significantly reduced in source rocks, rendering it difficult to accurately characterize paleo-productivity. Nevertheless, some geochemical and geological features involved in this study indicate high productivity levels. In this study, the phosphorus content (up to 1.59%) is greater than that in Post-Archean Average Australian Sedimentary rock (PAAS, 0.07%), suggesting that its primary productivity would be distinctly higher in a more reducing environment. In addition, high amounts of phosphorous biodetritus also occurred in the middle–upper part of the Chang 7^3 interval (Figures 4(c)–4(e)), supporting the above conclusion. Previous studies examined the paleo-productivity for the Ordos Basin in the Chang 7 interval ([16]; 218–2767 g/(m^2·a)) and concluded that the productivity at that time belonged to the eutrophic–hypertrophic lake type, which was significantly higher than the eutrophic lake water during the hydrocarbon source rock development in other basins in

Table 6: Quantitative calculation of the paleo-productivity of Chang 7^3 and Chang 8 intervals from well DP1 in the western Ordos Basin. The parameters of porosity and proportion of aquatic organisms derived from Wang [16] and the sedimentation rate refers to Chen et al. [19].

Member	Depth (m)	Density (g/cm^3)	TOC (%)	Porosity (%)	Sedimentation rate (cm/1000a)	Proportion of aquatic organisms	Paleo-productivity (g/m^2·a)
Chang 7^3	2743.96	2.47	5.25	0.42	1.30	0.73	1691.45
	2744.57	2.53	4.50	0.42	1.30	0.73	1484.83
	2745.24	2.44	6.02	0.42	1.30	0.73	1913.04
	2747.34	2.33	7.34	0.42	1.30	0.73	2228.60
	2747.22	2.35	9.21	0.42	1.30	0.73	2814.06
	2751.96	2.42	9.99	0.42	1.30	0.73	3141.62
	2756.18	2.49	4.31	0.42	1.30	0.73	1399.20
	2750.97	2.53	7.27	0.42	1.30	0.73	2395.97
	2757.09	2.49	5.24	0.42	1.30	0.73	1699.65
	2759.98	2.44	6.14	0.42	1.30	0.73	1950.09
	2762.68	2.81	7.40	0.42	1.30	0.73	2709.35
	2766.89	2.51	6.27	0.42	1.30	0.73	2045.85
	2767.92	2.49	5.61	0.42	1.30	0.73	1816.81
	2768.99	2.47	4.03	0.42	1.30	0.73	1295.69
	2770.86	2.47	5.02	0.42	1.30	0.73	1612.25
	2771.96	2.48	6.30	0.42	1.30	0.73	2031.24
	2773.01	2.45	6.69	0.42	1.30	0.73	2134.19
	2776.83	2.47	5.77	0.42	1.30	0.73	1855.19
	2777.59	2.41	2.61	0.42	1.30	0.73	818.98
Chang 8	2778.18	2.58	0.63	0.42	1.30	0.73	211.98
	2778.67	2.64	0.53	0.42	1.30	0.73	182.23
	2779.34	2.63	0.59	0.42	1.30	0.73	202.35
	2781.10	2.67	0.80	0.42	1.30	0.73	277.58
	2781.57	2.64	0.50	0.42	1.30	0.73	172.16
	2784.03	2.68	1.47	0.42	1.30	0.73	513.33

China (e.g., Songliao and Bohai Bay basins, 32.87–2460 g/(m^2·a)). It has been reported that the paleo-productivity was high in the southwest and low in the northeast and the paleo-productivity in Chang 7^3 period was considerably larger than the Chang 7^1 and Chang 7^2 periods [16]. In conclusion, the Chang 7^3 interval in this study had high paleo-productivity, which might also be the main material source of extreme organic matter deposition and accumulation.

5.3. Extreme Organic Matter Enrichment during the Chang 7^3 Interval. Organic matter enrichment has been considered to be primarily controlled by productivity and preservation over the past few decades [71]. Large-scale organic-rich marine shale sedimentation requires two important conditions: high paleo-productivity in surface water and oxygen depletion in bottom water [72]. Contrastingly, the continental lacustrine basin is smaller than the marine basin in the area, resulting in far less water circulation in lacustrine basin. The sedimentation of organic-rich lacustrine shale is mainly classified into two models: lake water stratification and lacustrine transgression [73]. The present study, referring to the Chang 7^3 sub-member, may be related to the lacustrine transgression model.

During the Chang 8 period, lake water was dominated by a shallow water delta environment based on sedimentary feature (Figure 4(a)), which made it difficult to achieve high paleo-productivity due to high-energy shallow water environment. Moreover, it was difficult to preserve organic matter from phytoplankton in surface water because of high plant debris input, and abundant terrigenous detritus will dilute the concentration of organic matter. Therefore, the sediments of the Chang 8 member have a relatively low TOC content. In the Chang 7^3 stage, the lake level rose rapidly, which changed the sedimentary environment of the Mahuangshan area from delta facies to semi-deep–deep lake facies. The abundant nutrient-rich water brought by lacustrine transgression would enhance surface primary productivity. For instance, the high TOC Chang 7^3 shale generally has high nutrient element content at well JH4 [15]. Because the study area was close to the Alashan ancient block in the western margin of the basin, it received terrestrial organic matter imports, which further increased the organic matter content of the Chang 7^3 sediments (Figure 13). For example, the organic matter found in this study generally has a high humic content (Figure 6). In contrast, these terrestrial inputs destroyed anoxic conditions and consumed organic matter.

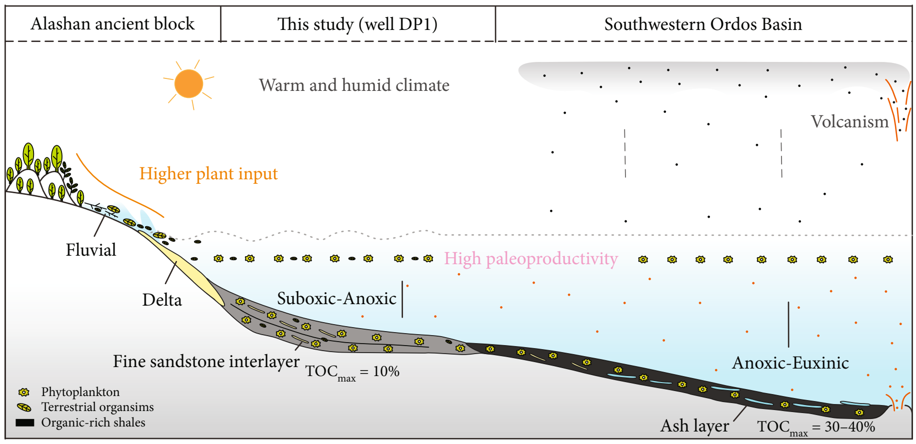

Figure 13: Mode of extreme organic matter enrichment during the Chang 7^3 interval in the Ordos Basin. The transect represents the basin from northwest (shallow) to southeast (deep).

Sedimentological studies from 10 wells in the north of the Jiyuan area (including wells Y66 and Feng6) show that delta front–pre-delta deposits are primarily developed in this area, gradually transitioning to a lacustrine environment in the southeastern direction [74]. Furthermore, there was a lack of volcanic activity in this region that could promote paleo-productivity. Therefore, although the study area was deposited in a semi-deep–deep lake environment, other environmental factors related to organic matter enrichment were poorer than those in the central and southern basins.

In summary, ultra-high surface primary productivity inspired by warm, humid conditions and lake transgression during the Chang 7^3 interval is the predominant controlling factor for extreme organic matter enrichment, although suboxic–anoxic bottom water also provided relatively satisfactory preservation conditions (Figure 13). It is worth noting that the sedimentary settings were different from those in the central or southern areas of the Ordos Basin, where there was ultra-high productivity, strongly anoxic–euxinic bottom water, and volcanic activity simultaneously [43]. Ultimately, the abundance and type of organic matter in the Mahuangshan area are worse than those in other areas (TOC>30–40%).

5.4. Implication for Shale Oil Exploration. The Chang 7 member is dominated by high TOC, type II kerogen, and moderate thermal maturation across the entire Ordos Basin. Therefore, this set of organic-rich shales is considered the main source rock for the Mesozoic oil and gas reservoirs. In particular, many sets of sand bodies have developed in the overlying Chang 6, Chang 7^1, Chang 7^2 (deep-water gravity flow reservoir), and the underlying Chang 8 members [75]. These sand bodies are in lateral contact with high-quality source rocks in a large area, which is beneficial for hydrocarbon expulsion and accumulation from the Chang 7 organic-rich shales and reservoir formation. The samples collected in this study show that yellow liquid light oil seeped out from the Chang 7^3 sub-member and upper Chang 8 member (Figure 3(f)). Similar results have been reported for other places [76]. In this study, shales containing a high proportion of terrigenous organic matter may be more favorable for the formation of light oil than those containing aquatic organic matter [23, 77]. Thus, there is strong shale oil exploration potential in the Chang 7^3 sub-member and its adjacent horizons in the Ordos Basin.

The practice of shale oil exploration and exploitation in North America displayed that the shale oil exploration potential only exists when the oil saturation index (OSI, $S_1/(100 \times \text{TOC})$) of the shale rock series is more than 100 mg/g [78]. In the well DP1, the OSI ranges from 16.39–107.91 mg/g, with an average of 55.78 mg/g (Table 1). Except for one sample of the Chang 8 member and the middle part of the Chang 7^3 sub-member, each of which exceeds 100 mg/g, most samples are lower than the exploration threshold and belong to the middle oil-bearing grade [49], indicating that this area is not suitable for shale oil exploration. Meanwhile, the OSI data from the Bingchang area in the southern Ordos Basin show that the gray–brown laminated, thin-bedded, and massive tuff and interbedded tuffaceous (argillaceous) siltstone is characterized by a high OSI ranging from 96 to 380 mg/g (average = 200 mg/g), indicating potential for shale oil. Therefore, although the Chang 7^3 shales in the Mahuangshan area are of high-quality source rock, compared with the better-quality source rock in the southern Ordos Basin, they have poorer shale oil exploitation potential. However, the Chang 7^3 sub-member in the study area is currently in the peak stage of the oil generation window, and it has a good spatial configuration relationship with well-developed sand bodies in the vertical direction, such as the Chang 6 + 8 member [75]. Therefore, it is more appropriate to study this layer as a conventional source rock in the study area. The deep lake areas that were deposited in extensive anoxic–euxinic bottom water and had extremely high primary productivity might be the key areas for shale oil exploration.

6. Conclusions

As the main source rock of Mesozoic hydrocarbon reservoirs in the Ordos Basin, the Late Triassic Chang 7^3 organic-rich shale plays an important role in regional oil and gas exploration. In the well DP1, sedimentology and geochemistry were used to reveal the source rock evaluation and extreme organic matter enrichment of the Chang 7^3 interval by using the well DP1 in the Mahuangshan area, the central Tianhuan Depression of the Ordos Basin. The main conclusions are as follows:

(1) The Chang 7^3 sub-member in the study area was deposited in a semi-deep–deep lake environment with a strong terrigenous input. This shale has a relatively high organic matter abundance (up to 10.60%). The primary organic matter type is type II, containing a high proportion of humic components. Combined with the moderate thermal maturation and a high hydrocarbon generation potential index ($S_1 + S_2$), this study proposes that the Chang 7^3 sub-member is an excellent source rock

(2) The high organic matter content of the Chang 7^3 sub-member was primarily controlled by ultra-high primary productivity (equal to hypereutrophic lakes) in surface water and lake transgression under warm and humid conditions. The higher salinity and relatively anoxic bottom water improved the preservation of organic matter. Relatively strong terrigenous input and less volcanic activities are the leading reasons for the lower organic matter abundance in the Mahuangshan area than in the deep lakes in the central and southern Ordos Basin

(3) The OSI (<100 mg/g) of most samples in the Chang 7^3 sub-member is lower than the threshold for shale oil exploitation; thus, this set of organic-rich shale is not a priority development horizon. Further shale oil exploration should emphasize anoxic, even euxinic deep lake areas with high organic matter content

Data Availability

The data has been included in the manuscript.

Conflicts of Interest

The authors declared no potential conflicts of interest with respect to the research, authorship, and/or publication of this article.

Acknowledgments

This work was supported by the National Natural Science Foundation of China (Grant No. 42172119), Chongqing Research Program of Basic Research and Frontier Technology (Grant No. cstc2021jcyj-msxmX0023), and the Fundamental Research Funds for the Central Universities (Grant No. 2021CDJQY-028).

References

[1] Z. J. Jin, G. P. Wang, G. X. Liu et al., "Research progress and key scientific issues of continental shale oil in China," *Acte Petrolei Sinica*, vol. 42, no. 7, pp. 821–835, 2021, (in Chinese with English abstract).

[2] R. J. Hill, E. T. Zhang, B. J. Katz, and Y. C. Tang, "Modeling of gas generation from the Barnett Shale, Fort Worth Basin, Texas," *AAPG Bulletin*, vol. 91, no. 4, pp. 501–521, 2007.

[3] D. M. Jarvie, "Shale resource system for oil and gas: Part2-shale oil resource systems," *AAPG Memoir*, vol. 97, pp. 89–119, 2012.

[4] B. Miller, J. Paneitz, M. Mullen, R. Meijs, K. Tunstall, and M. Garcia, "The successful application of a compartmental completion technique used to isolate multiple hydraulic-fracture treatments in Horizontal Bakken Shale Wells in North Dakota," *Paper presented at the SPE Annual Technical Conference and Exhibition*, 2008, p. 116469, 2008.

[5] J. Mullen, "Petrophysical characterization of the Eagle Ford shale in South Texas," in *Paper presented at the Canadian Unconventional Resources and International Petroleum Conference*, Calgary, Alberta, Canada, October 2010.

[6] H. Wu, W. Hu, Y. Wang et al., "Depositional conditions and accumulation models of tight oils in the middle Permian Lucaogou Formation in Junggar Basin, northwestern China: new insights from geochemical analysis," *AAPG Bulletin*, vol. 105, no. 12, pp. 2477–2518, 2021.

[7] Q. Y. Liu, P. Li, Z. J. Jin et al., "Organic-rich formation and hydrocarbon enrichment of lacustrine shale strata: a case study of Chang 7 Member," *Science China Earth Sciences*, vol. 65, pp. 118–138, 2021.

[8] C. N. Zou, Z. Yang, S. S. Sun et al., ""Exploring petroleum inside source kitchen": shale oil and gas in Sichuan Basin," *Science China Earth Sciences*, vol. 63, no. 7, pp. 934–953, 2020.

[9] B. Liu, A. Bechtel, D. Gross, X. F. Fu, X. N. Li, and R. F. Sachsenhofer, "Middle Permian environmental changes and shale oil potential evidenced by high-resolution organic petrology, geochemistry and mineral composition of the sediments in the Santanghu Basin, Northwest China," *International Journal of Coal Geology*, vol. 185, pp. 119–137, 2018.

[10] M. W. Li, Z. H. Chen, X. X. Ma et al., "Shale oil resource potential and oil mobility characteristics of the Eocene-Oligocene Shahejie Formation, Jiyang Super-Depression, Bohai Bay Basin of China," *International Journal of Coal Geology*, vol. 204, pp. 130–143, 2019.

[11] J. H. Fu, W. Guo, S. X. Li, X. Y. Liu, D. X. Chen, and X. P. Zhou, "Characteristics and exploration potential of muti-type shale oil in the 7th Member of Yanchang Formation, Ordos Basin," *Natural Gas Geoscience*, vol. 32, no. 12, pp. 1749–1761, 2021, (in Chinese with English abstract).

[12] F. Q. Wang, X. Z. Wang, L. X. Zhang, H. J. Liu, and Y. Lei, "The shale gas resources estimation: An example from Mesozoic Triassic Yanchang Formation Member Chang 7, Ordos Basin," *Earth Science Frontier*, vol. 20, no. 3, pp. 240–246, 2013, (in Chinese with English abstract).

[13] H. Yang, J. H. Fu, X. S. Liu, and P. L. Meng, "Accumulation conditions and exploration and development of tight gas in the Upper Paleozoic of the Ordos Basin," *Petroleum Exploration and Development*, vol. 39, no. 3, pp. 315–324, 2012.

[14] J. H. Fu, S. X. Li, L. M. Xu, and X. B. Niu, "Paleo-sedimentary environmental restoration and its significance of Chang 7 Member of Triassic Yanchang Formation in Ordos Basin, NW China," *Petroleum Exploration and Development*, vol. 45, no. 6, pp. 998–1008, 2018.

[15] Q. Li, S. H. Wu, D. L. Xia, X. L. You, H. M. Zhang, and H. Lu, "Major and trace element geochemistry of the lacustrine organic-rich shales from the Upper Triassic Chang 7 Member in the southwestern Ordos Basin, China: implications for

paleoenvironment and organic matter accumulation," *Marine and Petroleum Geology*, vol. 111, pp. 852–867, 2020.

[16] L. Wang, *The Recovery of the Paleoproductivity in the Period of Chang 7 in Ordos Basin and Its Control Factor*, Master's thesis dissertation, Northwest University, 2015, (in Chinese with English abstract).

[17] K. Zhang, R. Liu, Z. J. Liu, B. L. Li, J. B. Han, and K. A. Zhao, "Influence of volcanic and hydrothermal activity on organic matter enrichment in the Upper Triassic Yanchang Formation, southern Ordos Basin, Central China," *Marine and Petroleum Geology*, vol. 112, p. 104059, 2020.

[18] Z. J. Xu, L. F. Liu, T. G. Wang et al., "Application of fluid inclusions to the charging process of the lacustrine tight oil reservoir in the Triassic Yanchang Formation in the Ordos Basin, China," *Journal of Petroleum Science and Engineering*, vol. 149, pp. 40–55, 2017.

[19] G. Chen, W. Z. Gang, Y. Z. Liu et al., "High-resolution sediment accumulation rate determined by cyclostratigraphy and its impact on the organic matter abundance of the hydrocarbon source rock in the Yanchang Formation, Ordos Basin, China," *Marine and Petroleum Geology*, vol. 103, pp. 1–11, 2019.

[20] J. J. Yang, *Tectonic Evolution and Oil and Gas Distribution in Ordos Basin*, Petroleum Industry Press, Beijing, 2002, (in Chinese).

[21] H. Yang, W. T. Dou, X. Y. Liu, and C. L. Zhang, "Analysis on sedimentary facies of Member 7 in Yanchang Formation of Triassic in Ordos Basin," *Acta Sedimentologica Sinica*, vol. 28, no. 2, pp. 254–263, 2010, (in Chinese with English abstract).

[22] Q. R. Meng and G. W. Zhang, "Timing of collision of the North and South China blocks: controversy and reconciliation," *Geology*, vol. 27, no. 2, pp. 123–126, 1999.

[23] B. Zhang, Z. G. Mao, Z. Y. Zhang et al., "Black shale formation environment and its control on shale oil enrichment in Triassic Chang 7 Member, Ordos Basin, NW China," *Petroleum Exploration and Development*, vol. 48, no. 6, pp. 1304–1314, 2021.

[24] S. T. Fu, J. L. Yao, S. X. Li, X. P. Zhou, and M. R. Li, "Enrichment characteristics and resource potential of continental shale oil in Mesozoic Yanchang Formation, Ordos Basin," *Petroleum Geology and Experiment*, vol. 42, no. 5, pp. 698–710, 2020, (in Chinese with English abstract).

[25] Z. M. Li, G. L. Tao, M. W. Li et al., "Discussion on prospecting potential of shale oil in the 3rd sub-member of the Triassic Chang 7 member in Binchang block, southwestern Ordos Basin," *Oil and Gas Geology*, vol. 40, no. 3, pp. 558–570, 2019, (in Chinese with English abstract).

[26] Y. Zhang, Z. W. Liao, Z. G. Wu et al., "Climate change controls on extreme organic matter enrichment in Late Permian marine–terrestrial transitional shales in Guizhou, South China," *Journal of Petroleum Science and Engineering*, vol. 218, p. 111062, 2022.

[27] B. P. Tissot and D. H. Welte, *From Kerogen to Petroleum. In Petroleum Formation and Occurrence*, Springer, Berlin, Heidelberg, 1984.

[28] J. Espitalié, M. Madec, B. Tissot, J. Mennig, and P. Leplat, "Source rock characterization method for petroleum exploration," *Offshore Technology Conference*, 1977, p. 2935, 1977.

[29] K. E. Peters and M. R. Cassa, "Applied source rock geochemistry," in *The Petroleum System-from Source to Trap*, L. B. Magoon and W. G. Dow, Eds., vol. 60, pp. 93–120, AAPG Memoir, 1994.

[30] S. H. Huang, *Geochemical Characteristics and Paleoenvironmental Analysis of the Chang 7 Shale in Feng 75 Well Ordos Basin*, Master's Dissertation, China University of Geosciences, 2020, (in Chinese with English abstract).

[31] D. F. Wang, M. Liu, W. G. Yang, and L. Liu, "Distribution characteristics of dark mudstone and geochemical characteristics in Chang 7 of Yanchang Formation in Northern Jiyuan, Ordos Basin," *Journal of Mineralogy and Petrology*, vol. 36, no. 2, pp. 92–98, 2016, (in Chinese with English abstract).

[32] L. M. Ji, J. F. Li, M. Z. Zhang et al., "Effects of lacustrine hydrothermal activity on the organic matter input of source rocks during the Yanchang period in the Ordos Basin," *Marine and Petroleum Geology*, vol. 125, article 104868, 2021.

[33] C. He, L. M. Ji, A. Su et al., "Source-rock evaluation and depositional environment of black shales in the Triassic Yanchang Formation, southern Ordos Basin, north-central China," *Journal of Petroleum Science and Engineering*, vol. 173, pp. 899–911, 2019.

[34] W. Z. Zhang, H. Yang, W. W. Yang, K. Wu, and F. Liu, "Assessment of geological characteristics of lacustrine shale oil reservoir in Chang 7 Member of Yanchang Formation, Ordos Basin," *Geochimica*, vol. 44, no. 5, pp. 505–515, 2015, (in Chinese with English abstract).

[35] Standardization Committee of Petroleum Geological Exploration, *Geochemical evaluation method of continental source rocks in China: SY/T 5735-1995 [M]*, Petroleum Industry Press, 1995, in Chinese.

[36] J. W. Cui, R. K. Zhu, S. Li, Y. L. Qi, X. Z. Shi, and Z. G. Mao, "Oil and gas resources of shale formation orderly accumulation and coexistence as well as its prospecting significance: a case study of Chang 7 shale formation in Ordos Basin," *Geological Bulletin of China*, vol. 30, no. 7, pp. 982–996, 2019, (in Chinese with English abstract).

[37] L. M. Ji, *The Oil-Source Correlation, Biological Source and Paleo-Climate Studies of Triassic Source Rocks in Xifeng Area of East Gansu Province*, Doctoral dissertation, China University of Geoscience, 2018, (in Chinese with English abstract).

[38] Q. F. Kong, "The organic maceral characteristic of Yanchang source rock in Ordos Basin," *Xinjiang Petroleum Geology*, vol. 2, pp. 163–166, 2007, (in Chinese with English abstract).

[39] Z. L. Ren, W. H. Li, Y. Liang et al., "Tight oil reservoir formation conditions and main controlling factors of Yanchang Formation in southeastern Ordos Basin," *Oil and Gas Geology*, vol. 35, no. 2, pp. 190–198, 2014, (in Chinese with English abstract).

[40] C. L. Zhang, L. Zhang, D. S. Chen et al., "Provenance and parent-rock types of Member 7 of Yanchang Formation (Triassic), Ordos Basin," *Acta Sedimentologica Sinica*, vol. 31, no. 3, pp. 430–439, 2013, (in Chinese with English abstract).

[41] R. G. Wang, W. H. Li, Y. Y. Liao, Y. Q. Guo, and H. W. Liu, "Provenance analysis of Chang 7 Member of Triassic Yanchang Formation in Ordos Basin," *Geological Bulletin of China*, vol. 32, no. 4, pp. 671–684, 2013, (in Chinese with English abstract).

[42] Q. Zheng, Q. Liu, X. Liang et al., "Sedimentary facies analysis of the Chang 7 Member of the Upper Triassic Yanchang Formation in the Ordos Basin, NW China," *Journal of Stratigraphy*, vol. 44, no. 1, pp. 35–45, 2020.

[43] X. L. Yuan, S. H. Lin, Q. Liu et al., "Lacustrine fine-grained sedimentary features and organicrich shale distribution pattern: a

case study of Chang 7 Member of Triassic Yanchang Formation in Ordos Basin, NW China," *Petroleum Exploration and Development*, vol. 42, no. 1, pp. 37–47, 2015.

[44] B. Jones and D. A. Manning, "Comparison of geochemical indices used for the interpretation of palaeoredox conditions in ancient mudstones," *Chemical Geology*, vol. 111, no. 1–4, pp. 111–129, 1994.

[45] S. M. McLennan, "Relationships between the trace element composition of sedimentary rocks and upper continental crust," *Geochemistry, Geophysics, Geosystems*, vol. 2, no. 4, 2001.

[46] T. W. Lyons, J. P. Werne, D. J. Hollander, and R. W. Murray, "Contrasting sulfur geochemistry and Fe/Al and Mo/Al ratios across the last oxic–to–anoxic transition in the Cariaco Basin, Venezuela," *Chemical Geology*, vol. 195, no. 1-4, pp. 131–157, 2003.

[47] G. Shields and P. Stille, "Diagenetic constraints on the use of cerium anomalies as palaeoseawater redox proxies: an isotopic and REE study of Cambrian phosphorites," *Chemical Geology*, vol. 175, no. 1–2, pp. 29–48, 2001.

[48] T. J. Algeo and J. S. Liu, "A re-assessment of elemental proxies for paleoredox analysis," *Chemical Geology*, vol. 540, p. 119549, 2020.

[49] Z. M. Li, X. Q. Rui, M. W. Li et al., "Characteristics of typical hybrid shale oil system in North America and its implications," *Journal of Jinlin University (Earth Science Edition)*, vol. 45, no. 4, pp. 1060–1072, 2015, (in Chinese with English abstract).

[50] Y. L. Zheng, Z. Q. Ma, and B. C. Wang, "Geochemistry characteristics and sedimentary environment of oil shale from the Eocene Bahuli Formation in Liushuhe Basin, Heilongjiang Province," *Journal of Palaeogeography*, vol. 17, no. 5, pp. 689–698, 2015, (in Chinese with English abstract).

[51] W. Yuan, G. D. Liu, X. X. Zhou, L. M. Xu, and C. Z. Li, "Palaeoproductivity and organic matter accumulation during the deposition of the Chang 7 organic–rich shale of the Upper Triassic Yanchang Formation, Ordos Basin, China," *Geological Journal*, vol. 55, no. 4, pp. 3139–3156, 2020.

[52] W. Li and Z. G. Wen, "Characteristics of fine-grained sediments from the 7th Member of the Yanchang Formation in the Southwestern Ordos Basin," *Acta Geologica Sinica*, vol. 91, no. 5, pp. 1120–1129, 2017, (in Chinese with English abstract).

[53] H. H. Ma, C. Y. Liu, L. Zhang et al., "Geochemical Characteristics and Depositional Environment Implications of Sedimentary Rocks in the Chang 7 Member of Yanchang Formation in the Ordos Basin," *Geoscience*, vol. 33, no. 4, p. 872, 2019, (in Chinese with English abstract).

[54] J. Shi, Y. R. Zou, Y. L. Cai et al., "Organic matter enrichment of the Chang 7 member in the Ordos Basin: insights from chemometrics and element geochemistry," *Marine and Petroleum Geology*, vol. 135, p. 105404, 2022.

[55] J. Y. You, Y. Q. Liu, S. S. Song, D. W. Zhou, and Y. Y. Yang, "Characteristics and controlling factors of LORS from the Chang 7–3 section of the Triassic Yanchang Formation in the Ordos Basin," *Journal of Petroleum Science and Engineering*, vol. 197, p. 108020, 2021.

[56] D. K. Roy and B. P. Roser, "Climatic control on the composition of Carboniferous-Permian Gondwana sediments, Khalaspir Basin, Bangladesh," *Gondwana Reseach*, vol. 23, no. 3, pp. 1163–1171, 2013.

[57] H. Nesbitt and G. M. Young, "Early Proterozoic climates and plate motions inferred from major element chemistry of lutites," *Nature*, vol. 299, no. 5885, pp. 715–717, 1982.

[58] D. L. Li, *The geochemical characteristics and paleoenvironment reconstruction of Triassic Chang 7 oil shale in the south of Ordos Basin*, Doctoral dissertation, Chang'an University, 2018, (in Chinese with English abstract).

[59] R. X. Zhu, Z. Y. Yang, H. N. Wu et al., "Paleomagnetic constraints on the tectonic history of the major blocks of China during the Phanerozoic," *Science in China Series D: Earth Sciences*, vol. 41, no. 2, pp. 1–19, 1998.

[60] R. W. Murray, "Chemical-criteria to identify the depositional environment of chert general-principles and applications," *Sedimentary Geology*, vol. 90, no. 3-4, pp. 213–232, 1994.

[61] J. Q. Wang, C. Y. Liu, H. Li, T. T. Wu, and J. L. Wu, "Geochronology, potential source and regional implications of Tuff intervals in Chang-7 Member of Yanchang Formation, South of Ordos Basin," *Acta Sedimentologica Sinica*, vol. 35, no. 4, pp. 691–704, 2017, (in Chinese with English abstract).

[62] Y. L. Gao, Z. G. Wen, and W. Li, "Geochemical characteristics of lacustrine organic-rich fine-grained sedimentary rocks and its effects on the accumulation of tight oil: case study of Chang 7 Member of Triassic Yanchang Formation in Longdong area, Ordos Basin," *Nature Gas Geoscience*, vol. 30, no. 5, pp. 729–739, 2019, (in Chinese with English abstract).

[63] Q. H. Zheng, *The Characteristics of Origin and Oil Generation of Black Rock Series in Chang 7 Member of Yanchang Formation in Ordos Basin*, Doctoral dissertation, Northwest University, 2017, (in Chinese with English abstract).

[64] W. Wei and T. J. Algeo, "Elemental proxies for paleosalinity analysis of ancient shales and mudrocks," *Geochimica et Cosmochimica Acta*, vol. 287, pp. 341–366, 2020.

[65] Z. H. Ma, Q. S. Chen, Z. W. Shi, C. Wang, W. G. Du, and C. Y. Zhao, "Geochemistry of oil shale from Chang 7 reservoir of Yanchang Formation in South Ordos Basin and its geological significance," *Geological Bulletin of China*, vol. 35, no. 9, pp. 1550–1558, 2016, (in Chinese with English abstract).

[66] C. Wang, Q. X. Wang, G. J. Chen et al., "Petrographic and geochemical characteristics of the lacustrine black shales from the upper Triassic Yanchang formation of the Ordos Basin, China: implications for the organic matter accumulation," *Marine and Petroleum Geology*, vol. 86, pp. 52–65, 2017.

[67] Q. Jin, G. Y. Zhu, and J. Wang, "Deposition and distribution of high-potential source rocks in saline lacustrine environments," *Journal of China University of Petroleum (Edition of Natural Science)*, vol. 32, no. 4, p. 19, 2008, (in Chinese with English abstract).

[68] D. W. Kirkland and R. Evans, "Source-rock potential of evaporitic environment," *AAPG Bulletin*, vol. 65, no. 2, pp. 181–190, 1981.

[69] P. J. Müller and E. Suess, "Productivity, sedimentation rate, and sedimentary organic matter in the oceans—I. Organic carbon preservation," *Deep Sea Research Part A. Oceanographic Research Papers*, vol. 26, no. 12, pp. 1347–1362, 1979.

[70] K. Kelts, "Environments of deposition of lacustrine petroleum source rocks: an introduction," *Geological Society, London, Special Publications*, vol. 40, no. 1, pp. 3–26, 1988.

[71] R. V. Tyson, *The "Productivity versus preservation" controversy: cause, flaws, and resolution*, vol. 82, Society for Sedimentary Geology, Special Publication, 2011.

[72] M. A. Arthur and B. B. Sageman, "Marine black shales: depositional mechanisms and environments of ancient deposits," *Annual Review of Earth and Planetary Sciences*, vol. 22, no. 1, pp. 499–551, 1994.

[73] M. D. Picard, "Classification of fine-grained sedimentary rocks," *Journal of Sedimentary Research*, vol. 41, no. 1, pp. 179–195, 1971.

[74] Z. N. Jia, Y. M. Tian, M. Liu, W. Q. Li, and Z. Q. Lv, "Geochemical characteristics of mudstones in Chang-7 to Chang-8Members of the Yanchang Formation in the northern Jiyuan area and their geological significances," *Acta Mineralogica Sinica*, vol. 39, no. 5, pp. 549–557, 2019, (in Chinese with English abstract).

[75] J. L. Yao, X. Q. Deng, Y. D. Zhao, T. Y. Han, M. J. Chu, and J. L. Pang, "Characteristics of tight oil in Triassic Yanchang formation, Ordos Basin," *Petroleum Exploration and Development*, vol. 40, no. 2, pp. 161–169, 2013.

[76] X. Y. Liu, W. W. Yang, S. X. Li, L. Sun, and R. Chang, "Occurrence states and quantitative characterization of lacustrine shale oil from Yanchang Formation in Ordos Basin," *Natural Gas Geoscience*, vol. 32, no. 12, pp. 1762–1770, 2021, (in Chinese with English abstract).

[77] Z. W. Liao, X. F. Liu, D. Z. Song et al., "Micro-structural damage to coal induced by liquid CO_2 phase change fracturing," *Natural Resources Research*, vol. 30, no. 2, pp. 1613–1627, 2021.

[78] D. M. Jarvie, "Components and processes affecting producibility and commerciality of shale resource systems," *Geologica Acta: an international earth science journal*, vol. 12, no. 4, pp. 307–325, 2014.